Polarization transfer in relativistic magnetized plasmas

Jean Heyvaerts, Christophe Pichon, Simon Prunet, Jérôme Thiébaut

Monthly Notices
of the
ROYAL ASTRONOMICAL SOCIETY

MNRAS **430,** 3320–3349 (2013) doi:10.1093/mnras/stt135

Polarization transfer in relativistic magnetized plasmas

Jean Heyvaerts,[1,2]★ Christophe Pichon,[1,3]★ Simon Prunet[1] and Jérôme Thiébaut[1]

[1]*Institut d'Astrophysique de Paris, UMR 7095, CNRS, UPMC Univ. Paris VI, 98 bis boulevard Arago, 75014 Paris, France*
[2]*Observatoire Astronomique, Université de Strasbourg, CNRS, UMR 7550, 11 rue de l'Université, 67000 Strasbourg, France*
[3]*CEA Saclay, DSM/IPhT, Bâtiment 774, 91191 Gif-sur-Yvette, France*

Accepted 2013 January 18. Received 2013 January 17; in original form 2012 November 30

ABSTRACT

The polarization transfer coefficients of a relativistic magnetized plasma are derived. These results apply to any momentum distribution function of the particles, isotropic or anisotropic. Particles interact with the radiation either in a non-resonant mode when the frequency of the radiation exceeds their characteristic synchrotron emission frequency or quasi-resonantly otherwise. These two classes of particles contribute differently to the polarization transfer coefficients. For a given frequency, this dichotomy corresponds to a regime change in the dependence of the transfer coefficients on the parameters of the particle's population, since these parameters control the relative weight of the contribution of each class of particles. Our results apply to either regimes as well as the intermediate one. The derivation of the transfer coefficients involves an exact expression of the conductivity tensor of the relativistic magnetized plasma that has not been used hitherto in this context. Suitable expansions valid at frequencies much larger than the cyclotron frequency allow us to analytically perform the summation over all resonances at high harmonics of the relativistic gyrofrequency.

The transfer coefficients are represented in the form of two-variable integrals that can be conveniently computed for any set of parameters by using Olver's expansion of high-order Bessel functions. We particularize our results to a number of distribution functions, isotropic, thermal or power law, with different multipolar anisotropies of low order, or strongly beamed. Specifically, earlier exact results for thermal distributions are recovered. For isotropic distributions, the Faraday coefficients are expressed in the form of a one-variable quadrature over energy, for which we provide the kernels in the high-frequency limit and in the asymptotic low-frequency limit. An interpolation formula extending over the full energy range is proposed for these kernels. A similar reduction to a one-variable quadrature over energy is derived at high frequency for a large class of anisotropic distribution functions that may form a basis on which any smoothly anisotropic distribution could be expanded.

Key words: plasmas – polarization – radiative transfer – galaxies: magnetic fields.

1 INTRODUCTION AND MOTIVATION

The transfer of the intensity and polarization of radiation propagating in a relativistic magnetized plasma has been a long standing problem which still remains incompletely solved. Its potential diagnostic applications have long been known (Jones & O'Dell 1977; Cioffi & Jones 1980) and it has recently attracted renewed interest (Brentjens & de Bruyn 2005; Thiébaut et al. 2010) in connection with the study of the magnetic field structure of synchrotron emitting objects where the high-energy emitting particles may constitute the bulk of the plasma. Polarization data constrain the structure of geometrically complex sources and of their magnetospheres. Astrophysical environments such as the vicinity of the central black hole in the Milky Way (Agol 2000; Beckert 2003; Shcherbakov 2011), jet-sources, Galactic (Stirling et al. 2004) or extragalactic (Homan & Wardle 2004), pulsars (Kanbach et al. 2003; Dyks, Harding & Rudak 2004; Petri & Kirk 2005; Mc Donald et al. 2010; Yuen et al. 2012) or discs around black holes (Dovciak et al. 2008) have been studied by these methods. The perspectives of using polarization data to constrain magnetic fields have improved strongly by the deployment of low frequency array (Beck 2009), and will

★ E-mail: jean.heyvaerts@astro.unistra.fr (JH); pichon@iap.fr (CP)

blossom with the advent of square kilometer array (Carilli & Rawlings 2004; Dewdney, Schilizzi & Lazio 2009), ranging from the largest scales (Feretti & Johnston-Hollitt 2004; Gaensler, Beck & Feretti 2004) to the smallest ones (Bicknell, Jones & Lister 2004).

Using polarization data for the reconstruction of the magnetic field distribution in volume from multiwavelength observations of relativistically hot astrophysical media rests on the availability of good polarization transfer codes and on the knowledge of the transfer coefficients that would modify the intensity and the polarization of light as it propagates in the medium. Synchrotron radiation plays an important role in the emission of magnetized high-energy sources. The polarization properties of its emission and absorption caused by the high-energy population are well known. The non-dissipative transfer coefficients of Faraday rotation and Faraday conversion from circular to linear polarization have been more difficult to derive. Substantial progress has nevertheless been achieved in time (Trubnikov 1958; Zhelezniakov 1967; Sazonov 1969b; Melrose 1997a; Shcherbakov 2008; Huang & Shcherbakov 2011). However, the polarization transfer coefficients for high harmonic numbers have not been generally expressed yet in a manner similar to the dissipative transfer coefficients that involve, for any given distribution function, the integral of the product of some derivative of it with a well-defined energy- and direction-dependent kernel. Such an expression would be most useful for use in data inversion codes.

In this paper, we obtain such expressions for the polarization transfer coefficients in a relativistic homogeneous magnetized plasma for any distribution function and provide efficient means to calculate the general two-variable kernel. These expressions are reduced to simple one-variable quadratures for isotropic distributions and for a large class of non-isotropic ones as well. The derivation of these results parallels that of dissipative transfer coefficients. It is based on an expression of the high-frequency (HF) conductivity tensor of a magnetized relativistic plasma that has not been hitherto used in this context and involves, at some late stage of the derivation, well-justified approximations that allow us to explicitly sum series of principal parts in the limit of large harmonic numbers. Our results are shown to exactly coincide with previously known exact results in the case of thermal distributions.

Section 2 summarizes the basics of polarized radiation transfer in a uniformly magnetized medium. Section 3 presents in anticipation the end results of our derivation of the polarization transfer coefficients as a double regular quadrature and illustrates it for isotropic and anisotropic distributions, where it can sometimes be reduced to a single quadrature. This unconventional presentation has been chosen because the derivation of these results from those in Section 2, which is carried in Sections 4 and 5, is mathematical in some respects, as many previous contributions to this subject (Westfold 1959; Sazonov 1969b; Melrose 1997d; Swanson 2002). The reader who would like to closely follow the derivations presented in Sections 4 and 5 is invited to consult the series of appendices that are available in the online version of this paper only. Sections 4 and 5 can be skipped on a first read. Section 6 focuses on analytical results applicable to isotropic distribution functions in the low-frequency (LF) limit. Section 7 wraps up.

2 FORMULATION

This section briefly establishes ab initio some known results concerning the description of polarized radiation transfer in a uniformly magnetized medium and the associated derivation of the HF electrical conductivity from which the elements of the transfer matrix are obtained. Meanwhile, we set our notations and specify the nature of the large harmonic number approximation on which this work is based.

2.1 Description of polarization transfer

The polarization properties of transverse electromagnetic radiation are represented by a column vector of four Stokes parameters, $\boldsymbol{I} = {}^{\mathrm{T}}(I, Q, U, V)$, ${}^{\mathrm{T}}M$ denoting the transpose of the matrix M. The Stokes vector $\boldsymbol{I}$ depends on the frequency and direction of propagation of the radiation, as well as on the point in space and on the time at which it is observed. In the limit where the frequency is higher than any gyrofrequency, the Stokes vector satisfies a radiative transfer equation in which the generalized emission coefficient is a four-component column vector $\boldsymbol{W} = {}^{\mathrm{T}}(W_I, W_Q, W_U, W_V)$ and the generalized absorption coefficient is a 4×4 transfer matrix. This transfer equation can be written, for radiation of frequency ω and group velocity (based on an isotropic mean conductivity) $\boldsymbol{v}_g$ as

$$\left(\partial_t + \boldsymbol{v}_g \cdot \nabla\right) \begin{pmatrix} I \\ Q \\ U \\ V \end{pmatrix} = \begin{pmatrix} W_I \\ W_Q \\ W_U \\ W_V \end{pmatrix} - \begin{pmatrix} K_{II} & K_{IQ} & K_{IU} & K_{IV} \\ K_{IQ} & K_{II} & K_{QU} & K_{QV} \\ K_{IU} & -K_{QU} & K_{II} & K_{UV} \\ K_{IV} & -K_{QV} & -K_{UV} & K_{II} \end{pmatrix} \begin{pmatrix} I \\ Q \\ U \\ V \end{pmatrix}. \tag{1}$$

The four matrix elements K_{II}, K_{IQ}, K_{IU}, K_{IV} and the emission column vector $\boldsymbol{W}$ result from dissipative effects. The emission column vector $\boldsymbol{W}$ represents the emission rate and polarization of the spontaneously emitted radiation. The elements K_{QU}, K_{QV}, K_{UV} of the transfer matrix result from non-dissipative effects caused by the slowly varying phase difference between different transverse components of the electric vector of the radiation. The elements of the matrix in equation (1) can be expressed in terms of the components of the HF conductivity tensor $\boldsymbol{\sigma}(\boldsymbol{k}, \omega)$. Equation (1) has been established by a number of authors and by different methods (Sazonov & Tsytovitch 1968; Heyvaerts 1969; Zheleznyakov, Suzorov & Shaposhnikov 1974). A direct derivation of the absorption-like term is presented below. The derivation of the emission term is less straightforward (Sazonov & Tsytovitch 1968).

Since the wavelengths of the plasma eigenmodes of a given frequency ω do not differ by much from each other at HF, their phase difference evolves slowly in space and time. As a result, the correlations between these phases, which determine the state of polarization, are

maintained over a length much longer than the wavelength, justifying a radiative transfer approach. When the plasma frequency ω_p exceeds by much the gyrofrequencies Ω_A of all particle species A, the wavelengths of the eigenmodes still differ by a little amount when $\omega \gg \Omega_A$ although the dispersion relation may depart from the vacuum one when ω is of the order of ω_p. In any other case, the difference of the phases of the eigenmodes evolves on a wavelength scale and the radiative transfer approach is inappropriate. Assuming that there are only two eigenmodes with transverse components, if their phases would be correlated at some point and time, the rapid growth of their difference would reduce this correlation to nothing in only a few wavelengths. Thus, the polarization state of radiation supported by modes of largely different wavelengths for a given frequency reduces to that of the sum of two mutually incoherent eigenmodes. Equation (1) is then only relevant in the HF limit, $\omega \gg \Omega_A$. It can be written in this form in the weakly anisotropic medium approximation, in which the wave dispersion is approximated by neglecting the longitudinal component of partially transverse eigenmodes (Zheleznyakov et al. 1974).

We now show how the elements of the absorption matrix relate to those of the conductivity tensor. We start from the propagation equation of the electric field $\boldsymbol{E}(\boldsymbol{r}, t)$, deduced from Maxwell's equations:

$$\frac{1}{c^2}\frac{\partial^2 \boldsymbol{E}}{\partial t^2} - \Delta \boldsymbol{E} + \mu_0 \frac{\partial \boldsymbol{J}}{\partial t} = 0. \tag{2}$$

Our equations are written in the MKSA system of units, where ε_0 is the dielectric permittivity of vacuum and μ_0 its magnetic permeability. The velocity of light in vacuum is $c = (\varepsilon_0 \mu_0)^{-1/2}$. In equation (2), $\boldsymbol{E}$ is the electric field and $\boldsymbol{J}$ the current density. The electric field is assumed to be transverse, so that div $\boldsymbol{E} = 0$, which is a good approximation at HF. The microscopic electric field is then Fourier expanded, its complex vectorial amplitude $\hat{\boldsymbol{E}}_{\boldsymbol{k},\omega}$ being regarded as slowly depending on space and time, which is equivalent to coarse graining in Fourier space. The electric current density $\boldsymbol{J}(\boldsymbol{r}, t)$ is similarly expanded. The phase, and possibly the amplitude, of the microscopic electric field is a random variable. Omitting the indices $\boldsymbol{k}$, ω for simplicity, each term of the Fourier expansion can be written as

$$\boldsymbol{E}(\boldsymbol{r}, t) = \hat{\boldsymbol{E}}(\boldsymbol{r}, t)\, \mathrm{e}^{\mathrm{i}(\boldsymbol{k}\cdot\boldsymbol{r} - \omega t)}. \tag{3}$$

The current in equation (2) is the sum of an induced current $\boldsymbol{J}'$, which results from the electric field $\boldsymbol{E}(\boldsymbol{r}, t)$ and a spontaneous current $\boldsymbol{J}''$, the microcurrent created by the individual plasma particles, which gives rise to spontaneous emission, while the induced current gives rise to the absorption-like term in equation (1). The latter part of the current is given in terms of the electric field by a linear non-local and causal conductivity tensor operator:

$$\boldsymbol{J}'(\boldsymbol{r}, t) = \int_0^\infty \mathrm{d}\tau \iiint \mathrm{d}^3 R \;\; \boldsymbol{\Sigma}(\boldsymbol{R}, \tau) \cdot \boldsymbol{E}(\boldsymbol{r} - \boldsymbol{R}, t - \tau). \tag{4}$$

In the weakly anisotropic medium approximation, the conductivity operator can be split into a scalar isotropic part, $\boldsymbol{\Sigma}_\mathrm{s}$, and a tensorial anisotropic part $\boldsymbol{\Sigma}_1$. The isotropic part may, for example, represent the dispersive properties of a cold population of relatively large density, neglecting the magnetization of these particles. An isotropic conductivity has no effect on the polarization but affects the propagation properties of electromagnetic waves. No component of the conductivity need to be separated out when the propagation is represented well enough by the vacuum dispersion relation. The tensorial anisotropic part consists of the anisotropic residual of the conductivity, not included in $\boldsymbol{\Sigma}_\mathrm{s}$, and of the conductivity of populations which negligibly contribute to the dispersive properties of the plasma waves. The frequency ω supposedly being much larger than all gyrofrequencies, the component $\boldsymbol{\Sigma}_1$ must be small. Its contribution to the dispersion properties may be neglected but it nevertheless contributes to the polarization transfer matrix.

The form of the electric field in equation (3) is inserted in equations (2) and (4). When acting on the imaginary exponential phase factor the operators ∂_t and ∇ are of orders ω and k, respectively, but when acting on the slowly varying amplitude $\hat{\boldsymbol{E}}(\boldsymbol{r}, t)$ they are of orders $1/T$ and $1/L$, T and L being the time and length scales on which $\hat{\boldsymbol{E}}$ varies, which are much longer than the wave period and wavelength. Only the terms of first order in $1/(\omega T)$ and $1/(kL)$ are retained. For consistency, this requires that $\hat{\boldsymbol{E}}(\boldsymbol{r} - \boldsymbol{R}, t - \tau)$ in equation (4) be expanded as

$$\hat{\boldsymbol{E}}(\boldsymbol{r} - \boldsymbol{R}, t - \tau) = \hat{\boldsymbol{E}}(\boldsymbol{r}, t) - \tau\, \partial_t \hat{\boldsymbol{E}} - (\boldsymbol{R} \cdot \nabla)\, \hat{\boldsymbol{E}}. \tag{5}$$

The time and space integrations in equation (4) then involve the Fourier transforms of $\boldsymbol{\Sigma}_\mathrm{s}$ and $\boldsymbol{\Sigma}_1$, $\sigma_\mathrm{s}(\boldsymbol{k}, \omega)$ and $\boldsymbol{\sigma}(\boldsymbol{k}, \omega)$ (no index 1), the latter being a tensor, and the derivatives of σ_s with respect to ω and $\boldsymbol{k}$. This results in

$$\left(\omega^2 - c^2 k^2 + \frac{\mathrm{i}\omega}{\varepsilon_0}\sigma_\mathrm{s}\right)\hat{\boldsymbol{E}} + \left(2\mathrm{i}\omega - \frac{1}{\varepsilon_0}\frac{\partial\,(\omega\sigma_\mathrm{s})}{\partial\omega}\right)\partial_t \hat{\boldsymbol{E}} + \left(\left(2\mathrm{i}c^2\boldsymbol{k} + \frac{\omega}{\varepsilon_0}\nabla_{\boldsymbol{k}}\sigma_\mathrm{s}\right)\cdot\nabla\right)\hat{\boldsymbol{E}} = -\frac{\mathrm{i}\omega}{\varepsilon_0}\boldsymbol{\sigma}(\boldsymbol{k}, \omega)\cdot\hat{\boldsymbol{E}}. \tag{6}$$

The term of dominant order in equation (6) is the first one. The two other terms on the left are of first order in $1/(\omega T)$ and $1/(kL)$ and the term on the right is also regarded as small. Equation (6) is satisfied at the dominant order when the factor of $\hat{\boldsymbol{E}}$ vanishes, which means that the electric field consists of fluctuations, the frequency of which is ω_k, the solution of the isotropic dispersion relation:

$$\omega^2 - c^2 k^2 + \frac{\mathrm{i}\omega}{\varepsilon_0}\sigma_\mathrm{s}(k, \omega) = 0. \tag{7}$$

The corresponding group velocity, $\boldsymbol{v}_g$, is obtained by differentiating equation (7) with respect to ω and k. When σ_s represents the dispersion due to a cold unmagnetized plasma, which we assume for simplicity, $\omega\sigma_\mathrm{s}$ does not depend on ω nor on k. With these simplifications, the three subdominant terms in equation (6) reduce to

$$\left(\partial_t + (\boldsymbol{v}_g \cdot \nabla)\right)\hat{\boldsymbol{E}} = -\frac{\boldsymbol{\sigma}(\boldsymbol{k}, \omega_k)\cdot\hat{\boldsymbol{E}}}{2\varepsilon_0}, \tag{8}$$

where the amplitude $\hat{\boldsymbol{E}}$, which slowly varies with position and time, is only non-vanishing when the wave vector $\boldsymbol{k}$ and the frequency ω_k are linked by the dispersion relation in equation (7). An equation for the correlation tensor of the electric field of this radiation, $\langle \hat{\boldsymbol{E}} \otimes \hat{\boldsymbol{E}}^* \rangle$, can be derived from equation (8) by tensorial multiplication by $\hat{\boldsymbol{E}}^*$, the superscript * denoting complex conjugation, and averaging over the statistical distribution of the phases (and possibly of the amplitudes) of the components of $\hat{\boldsymbol{E}}$. This operation is represented by brackets. The electric field supposedly being transverse, it pertains the plane perpendicular to the propagation direction $\boldsymbol{n}$ and may be represented by its components on two arbitrarily chosen unit basis vectors $\boldsymbol{e}_1$ and $\boldsymbol{e}_2$ in this plane. An intensity tensor with components I_{ij} relative to this basis that is proportional to the two-dimensional electric field correlation tensor must be defined such that it has the dimension of a specific intensity. We define the Stokes parameters of the radiation as being related to this intensity tensor by

$$I_{ij} \equiv v_g \frac{k^2 \mathrm{d}k}{\mathrm{d}\omega_k} \begin{pmatrix} \varepsilon_0 \langle \hat{E}_1 \hat{E}_1^* \rangle & \varepsilon_0 \langle \hat{E}_1 \hat{E}_2^* \rangle \\ \varepsilon_0 \langle \hat{E}_2 \hat{E}_1^* \rangle & \varepsilon_0 \langle \hat{E}_2 \hat{E}_2^* \rangle \end{pmatrix} = \begin{pmatrix} I + Q & U + \mathrm{i}V \\ U - \mathrm{i}V & I - Q \end{pmatrix}. \tag{9}$$

The transfer equation for the components I_{ij} can be deduced from equation (8) which writes, using the dummy index rule

$$\left(\partial_t + (\boldsymbol{v}_g \cdot \nabla)\right) I_{ij} = -\frac{1}{2\varepsilon_0} \left(\sigma_{ip}\delta_{jq} + \delta_{ip}\sigma_{jq}^*\right) I_{pq}. \tag{10}$$

By equation (9), the term on the right of equation (10) can be converted into the transfer matrix term in equation (1), some elements of which turn out to involve the Hermitian (dissipative) part of the conductivity while others involve its anti-Hermitian (non-dissipative) part. These parts are, respectively, defined by

$$\sigma_{ij}^H = \frac{1}{2}\left(\sigma_{ij} + \sigma_{ji}^*\right), \qquad \sigma_{ij}^A = \frac{1}{2}\left(\sigma_{ij} - \sigma_{ji}^*\right). \tag{11}$$

The elements of the transfer matrix in equation (1) are given in terms of these parts of the conductivity by

$$K_{II} = \frac{\mathcal{R}e\left(\sigma_{11}^H + \sigma_{22}^H\right)}{2\varepsilon_0}, \qquad K_{IQ} = \frac{\mathcal{R}e\left(\sigma_{11}^H - \sigma_{22}^H\right)}{2\varepsilon_0}, \qquad K_{IU} = \frac{\mathcal{R}e\left(\sigma_{12}^H\right)}{\varepsilon_0}, \qquad K_{IV} = \frac{\mathcal{I}m\left(\sigma_{12}^H\right)}{\varepsilon_0},$$
$$K_{QU} = \frac{\mathcal{R}e\left(\sigma_{12}^A\right)}{\varepsilon_0}, \qquad K_{UV} = \frac{\mathcal{I}m\left(\sigma_{22}^A - \sigma_{11}^A\right)}{2\varepsilon_0}, \qquad K_{QV} = \frac{\mathcal{I}m\left(\sigma_{12}^A\right)}{\varepsilon_0}. \tag{12}$$

These matrix elements refer to the components of the local conductivity for the wave vector $\boldsymbol{k}$ and frequency ω_k related to it by the dispersion relation in equation (7). The relations in equation (12) between the transfer coefficients and the elements of the conductivity matrix agree with those in Shcherbakov & Huang (2011) given the relation between conductivity and dielectric tensors for perturbations varying as in equation (3) and accounting for the fact, mentioned above, that their definition of the Stokes parameter V differs from ours by a sign.

The polarization properties of the synchrotron emission are well known, both in vacuum (Westfold 1959) and in a cold plasma (Tsytovitch 1950; Razin 1960; Ramaty 1968). The dissipative absorption coefficients K_{II}, K_{IQ}, K_{IU}, K_{IV} given in equation (12) in terms of the components of the Hermitian part of the conductivity have also been presented in the literature (Ginzburg & Sirovatskii 1969; Sazonov 1969a). These components can be calculated using the same well-known approximations that also provide the emission coefficient. The dissipative absorption can be derived from the emission by Einstein's coefficients method, ignoring dispersion (Wild et al. 1963), or not (Zhelezniakov 1967).

The non-dissipative coefficients K_{QU}, K_{UV}, K_{QV} have proved more difficult to calculate. This paper concentrates on their calculation in the case of ultrarelativistic plasma particles immersed in a static uniform magnetic field $\boldsymbol{B}_0$ and for frequencies of large harmonic number. The motion of the particles is described in the Vlasov approximation. We neglect the dispersive properties of a cold population that might be present, so that the dispersion relation (7) supposedly reduces to $\omega = ck$.

2.2 Formal solution for the HF conductivity tensor

The conductivity tensor is found by calculating the HF current $\boldsymbol{J}$ resulting from a HF electric field $\boldsymbol{E}$ by solving the linearized Vlasov equation for the perturbation $f(\boldsymbol{r}, \boldsymbol{p})$ of the distribution function,

$$\partial_t f + \boldsymbol{v} \cdot \nabla f + (q\boldsymbol{v} \times \boldsymbol{B}_0) \cdot \nabla_{\boldsymbol{p}} f = -q(\boldsymbol{E} + \boldsymbol{v} \times \boldsymbol{B}) \cdot \nabla_{\boldsymbol{p}} f_0, \tag{13}$$

where q is the charge (with its sign) of the particle species considered. In equation (13), $f_0(\boldsymbol{p})$ is the unperturbed homogeneous distribution function of the species considered, that only depends on the component $p_\parallel$ of the particle's momentum along the magnetic field and on the modulus $p_\perp$ of its component perpendicular to it, normalized to the density of particles, so that

$$\int_0^\infty \int_{-\infty}^{+\infty} 2\pi p_\perp \mathrm{d}p_\perp \mathrm{d}p_\parallel f_0(p_\perp, p_\parallel) = n, \tag{14}$$

where n is the volume density of this species of particles. The gradient with respect to position is denoted as ∇ and the gradient with respect to some other vectorial variable $\boldsymbol{u}$, such as the momentum $\boldsymbol{p}$, is denoted by $\nabla_{\boldsymbol{u}}$. The first three terms of equation (13) represent the time derivative of f following the unperturbed particle's motion, described by the position and momentum $\boldsymbol{r}(t')$ and $\boldsymbol{p}(t')$ of this particle at time t', following the unperturbed motion. At time t, the particle is at $\boldsymbol{r}$ with momentum $\boldsymbol{p}$. A standard procedure to obtain the perturbation f is by

then integrating in time the right-hand side term of equation (13) following the unperturbed particle's motion, as shown for example in the textbooks by Montgomery & Tidman (1964) or Ichimaru (1973). This gives

$$f(\boldsymbol{r},\,\boldsymbol{p},\,t) = -q\,\int_{-\infty}^{t} \mathrm{d}t'\,(\boldsymbol{E}(\boldsymbol{r}(t'),\,t') + \boldsymbol{v}(t')\times\boldsymbol{B}(\boldsymbol{r}(t'),\,t')\cdot\nabla_p f_0(\boldsymbol{p}(t')). \tag{15}$$

The integration is over all times t' earlier than t. The unperturbed motion is easily expressed in a frame where $\boldsymbol{B}_0$ is along the Z-axis so that $\boldsymbol{B}_0 = B_0\,\boldsymbol{e}_Z$ and the two unit vectors $\boldsymbol{e}_X$ and $\boldsymbol{e}_Y$ are perpendicular to it, but otherwise unspecified. The velocity of a particle can be written as

$$\boldsymbol{v} = v_\perp\,\cos\phi\,\boldsymbol{e}_X + v_\perp\,\sin\phi\,\boldsymbol{e}_Y + v_\parallel\,\boldsymbol{e}_Z\,, \tag{16}$$

where $v_\perp$ and $v_\parallel$ are conserved by the unperturbed motion, as are also the modulus p of the momentum, the associated Lorentz factor γ and the particle's pitch angle ϑ. The angle ϕ, the gyration angle of the particle, rotates in time at the synchrotron frequency Ω_*, which for non-relativistic particles reduces to the cyclotron frequency Ω. These frequencies, which have the sign opposite to that of the charge, s_q, depend on the rest mass m of the particles and are given by

$$\Omega_* = -\frac{q\,B_0}{\gamma\,m}\,, \qquad \Omega = -\frac{q\,B_0}{m}\,, \qquad \text{and} \qquad s_q = \mathrm{sign}(q). \tag{17}$$

At a time $t' = t - \tau$ earlier than t, the components of the velocity of a freely moving particle having at time t a gyration angle ϕ and a position X, Y, Z were

$$v_X(t-\tau) = v_\perp(t)\cos(\phi - \Omega_*\tau)\,, \qquad v_Y(t-\tau) = v_\perp(t)\sin(\phi-\Omega_*\tau)\,, \qquad v_Z(t-\tau) = v_\parallel(t). \tag{18}$$

The position of that particle at time $t-\tau$ was

$$X(t-\tau) = X - \frac{v_\perp}{\Omega_*}\,(\sin\phi - \sin(\phi-\Omega_*\tau))\,, \qquad Y(t-\tau) = Y + \frac{v_\perp}{\Omega_*}\,(\cos\phi - \cos(\phi-\Omega_*\tau))\,, \qquad Z(t-\tau) = Z - v_\parallel\,\tau. \tag{19}$$

The magnetic perturbation is related to the electric one by the Faraday equation, $\mathrm{curl}\,\boldsymbol{E} = -\partial_t\boldsymbol{B}$. The perturbation in the distribution function which develops as a result of an electric field perturbation such as that in equation (3) can be written as $f(\boldsymbol{r},\,\boldsymbol{p},\,t) = \hat{f}(\boldsymbol{p})\exp(\mathrm{i}(\boldsymbol{k}\cdot\boldsymbol{r} - \omega t)$. It depends linearly on the perturbation field by equation (15) and can be expressed in terms of operators acting on the unperturbed distribution function, such as the anisotropy operator D, defined by

$$D(f_0) = \left(v_\perp\frac{\partial f_0}{\partial p_\parallel} - v_\parallel\frac{\partial f_0}{\partial p_\perp}\right). \tag{20}$$

$D(f_0)$ vanishes for an isotropic distribution function. The wave vector $\boldsymbol{k}$ is taken to be in the $X-Z$ plane and has components $k_X = k\sin\alpha$ and $k_Z = k\cos\alpha$, the propagation angle α being comprised between 0 and π. When fully expanded, the solution for $\hat{f}$ can be written from equation (15) as

$$\hat{f}(\boldsymbol{p}) = -\frac{q}{\omega}\int_0^\infty \mathrm{d}\tau\,\exp\left(\mathrm{i}\left((\omega - k_\parallel v_\parallel)\,\tau - \frac{k_\perp v_\perp}{\Omega_*}(\sin\phi - \sin(\phi-\Omega_*\tau)\right)\right)$$
$$\times\left[(\hat{E}_X\cos(\phi-\Omega_*\tau) + \hat{E}_Y\sin(\phi-\Omega_*\tau)\left(\omega\frac{\partial f_0}{\partial p_\perp} + k_\parallel D(f_0)\right) + \hat{E}_Z\left(\omega\frac{\partial f_0}{\partial p_\parallel} - \cos(\phi-\Omega_*\tau)\,k_\perp D(f_0)\right)\right]. \tag{21}$$

The associated Fourier coefficient of the current density is the average value of $q\,\boldsymbol{v}$ weighted by $\hat{f}(\boldsymbol{p})$. Using the solution for $\hat{f}$ in equation (21), each component of the current appears to be a linear function of the electric field components $\hat{E}_X$, $\hat{E}_Y$ and $\hat{E}_Z$ from which the components of the conductivity tensor may be identified. Each one involves a fourfold integral on the variables $p_\parallel$, $p_\perp$, ϕ of the particle momentum and on the delay time τ. As can be seen in equation (21), integration over the delay time involves imaginary exponentials with an argument linear and trigonometric in τ. We refer to these integrals as phase integrals. Expanding the trigonometric functions of $(\phi - \Omega_*\tau)$ in the second line of equation (21) in imaginary exponentials, three phase integrals appear, that can be written as

$$P_\varepsilon(\omega, k_\perp, k_\parallel, \boldsymbol{v}) = \int_0^\infty \mathrm{d}\tau\;\exp\left(\mathrm{i}\left((\omega - k_\parallel v_\parallel)\tau - \frac{k_\perp v_\perp}{\Omega_*}(\sin\phi - \sin(\phi-\Omega_*\tau)) + \varepsilon(\phi-\Omega_*\tau)\right)\right). \tag{22}$$

The index ε may take the three values $(-1,\,0,\,+1)$, or $(-,\,0,\,+)$. At this point, it is necessary to take care of the sign of the charge, and to introduce dimensionless variables, simpler than those in equation (22), by

$$x = \frac{k_\perp v_\perp}{|\,\Omega_*\,|}\,, \qquad \sigma = \frac{\omega - k_\parallel v_\parallel}{|\,\Omega_*\,|}\,, \qquad u = \frac{\omega}{|\,\Omega\,|}\,, \qquad \sigma_0 = u\,\sin\alpha\,, \qquad \varpi = \frac{ck_\parallel - v_\parallel k}{|\,\Omega_*\,|}. \tag{23}$$

The variables x (not a coordinate), σ and u are all positive and usually large since $\omega = ck \gg |\Omega|$. The variable ϖ, which plays the role of an angular variable, may be positive or negative. The modulus of ϖ assumes values of the same order as σ. The properties of the variables ϖ and σ, which may replace $p_\parallel$ and $p_\perp$ as dynamical variables of freely moving particles, are detailed in Appendix A. From equation (21), the

current density can be written in terms of the three phase integrals as

$$\hat{\boldsymbol{J}} = -\frac{2\pi q^2}{\omega}\int_{-\infty}^{+\infty}\mathrm{d}p_\parallel\int_0^\infty p_\perp \mathrm{d}p_\perp\int_0^{2\pi}\frac{\mathrm{d}\phi}{2\pi}\;\left[v_\perp\cos\phi\,\boldsymbol{e}_X + v_\perp\sin\phi\,\boldsymbol{e}_Y + v_\parallel\,\boldsymbol{e}_Z\right]$$
$$\times\left[\frac{P_+ + P_-}{2}\left(\omega\frac{\partial f_0}{\partial p_\perp} + k_\parallel D(f_0)\right)\hat{E}_X + \frac{P_+ - P_-}{2\mathrm{i}}\left(\omega\frac{\partial f_0}{\partial p_\perp} + k_\parallel D(f_0)\right)\hat{E}_Y + \left(P_0\,\omega\frac{\partial f_0}{\partial p_\parallel} - \frac{P_+ + P_-}{2}\,k_\perp D(f_0)\right)\hat{E}_Z\right]. \tag{24}$$

3 RESULTS

We derive in Section 4 the components of the conductivity tensor for a relativistic plasma at frequencies much higher than the gyrofrequency and carry out two out of the four integrals involved in equations (22) and (24). In particular cases, the corresponding quadrature may be pursued one step farther. In this section, we anticipate the polarization transfer coefficients and illustrate them for isotropic and anisotropic distributions.

3.1 Dissipation-less polarization transfer coefficients

3.1.1 Quasi-exact expressions

We obtain in Section 4.4 a general expression for the Faraday rotation and conversion coefficients f and h, defined as $f = K_{QU}/c$ and $h = K_{UV}/c$, where K_{QU} and K_{UV} are given by equation (12). These coefficients can be explicitly written as in equations (86) and (87), which we reproduce here neglecting the principal value terms that are shown in Section 4.4 to be safely negligible when $\omega \gg \Omega$. These equations are therefore almost exact in this limit. We refer to them as being nearly exact or quasi-exact. They can be written as

$$f = -\frac{2\pi^2 s_q}{c}\,\frac{\omega_{\rm pr}^2\Omega^2}{\omega^3}\iint\frac{m^3c^3}{\sin^2\!\alpha}\,\mathrm{d}\varpi\,\mathrm{d}\sigma\;\;\varpi\,x\,\frac{\partial F_0}{\partial\sigma}\;\left[J'_\sigma(x)N_\sigma(x) + \frac{1}{\pi x}\right], \tag{25}$$

$$h = \frac{\pi^2}{c}\frac{\omega_{\rm pr}^2\Omega^2}{\omega^3}\iint\frac{m^3c^3}{\sin^2\!\alpha}\,\mathrm{d}\varpi\,\mathrm{d}\sigma\left[\frac{\partial F_0}{\partial\sigma}\left(x^2J'_\sigma(x)N'_\sigma(x) - \varpi^2J_\sigma(x)N_\sigma(x)\right) + \frac{1}{\pi}\left(\varpi\frac{\partial F_0}{\partial\varpi} - \sigma\frac{\partial F_0}{\partial\sigma}\right)\right]. \tag{26}$$

The particle's dynamical variables ϖ and σ, defined in equation (23), incorporate properties of the radiation of interest. Much of the dependence of f and h on the propagation angle α and on the frequency is in fact hidden in these variables. The distribution function F_0 is normalized to unity [in the sense of equation (75) below)], the particle density n being implicit in the square of the species' plasma frequency $\omega_{\rm pr}^2 = nq^2/m\varepsilon_0$. The integrals in equations (25) and (26) involve two-variable kernels in which one of the variables, σ, appears as a continuous Bessel function index. This index is larger than their argument x, as can be seen from equation (23), but possibly not much larger, which complicates the search for suitable approximations.

There are essentially two very different regimes, defined in Section 5, for the wave–particle interaction which we refer to as non-resonant (NR) and quasi-resonant (QR). Different particles make very different contributions to the transfer coefficients depending on whether they interact in the NR or in the QR regime. Equations (25) and (26) however encompass all regimes, being written in a form that does not require any regioning of the ϖ–σ domain for their evaluation. The domain of validity of specific approximations, NR or QR, to the functions in equations (25) and (26) is different and complementary (Fig. 6).

3.1.2 HF limit

It is shown in Section 5.1 that when the inequality

$$\frac{3\,\gamma^2\sin\alpha\;|\,\Omega\,|}{\omega} < 1 \tag{27}$$

holds true, only the NR domain, defined in that section, contributes to the transfer coefficients. For a given value of the Lorentz factor γ, the inequality (27) is satisfied when the radiation's frequency ω exceeds the characteristic synchrotron frequency $\omega_c(\gamma,\,\alpha)$ for particles of this energy travelling in the direction of the radiation (equation 101). We therefore refer to this situation as the HF limit. When all particles in the distribution interact with the wave in this regime, the integration on the NR domain actually extends over the full ϖ–σ domain. In this case, the Faraday coefficients f and h result from equations (115) and (119), expanded to the first non-vanishing order in Ω/ω:

$$f_{\rm HF} = 2\pi s_q\,\frac{\omega_{\rm pr}^2\Omega^2}{c\,\omega^3}\iint\frac{m^3c^3}{\sin^2\!\alpha}\mathrm{d}\varpi\,\mathrm{d}\sigma\;\;\left(\frac{\varpi\,x^2}{2\,(\sigma^2-x^2)^{3/2}}\right)\;\frac{\partial F_0}{\partial\sigma}. \tag{28}$$

$$h_{\rm HF} = -\,\pi\,\frac{\omega_{\rm pr}^2\Omega^2}{c\,\omega^3}\iint\frac{m^3c^3}{\sin^2\!\alpha}\,\mathrm{d}\varpi\,\mathrm{d}\sigma\;\;\left(\frac{2x^4(\sigma^2-x^2)+\sigma_0^2\,x^2(4\sigma^2+x^2)}{8\,(\sigma^2-x^2)^{7/2}}\right)\;\frac{\partial F_0}{\partial\sigma}. \tag{29}$$

Equations (28) and (29) do not assume isotropy of the distribution function F_0 but are only valid when the QR contribution can be neglected, which makes them less general than equations (25) and (26).

3.1.3 Medium frequency (MF): cutting through the QR domain

The integration over the NR domain cannot be extended to the full domain when the inequality in equation (27) is not satisfied for a non-negligible number of particles in the distribution. This arises in particular when the parameter on the left of equation (27) is of order unity, which we refer to as an MF situation. A slightly more sophisticated approach is then needed, which we now describe. The double quadratures in equations (28) and (29) should in this case be extended over the NR domain only and the contribution of the QR domain should be added to it. When it is not dominant, the integral over the QR domain may be approximately evaluated. Our proposed approximation rests on separating the NR from the QR domain, and expressing the integral over the QR one by using a very simple approximation. The boundary $\mathcal{B}_{\rm QR}$ between the NR and QR regions is where the variable g defined in equation (94) below is near unity. Since $x \approx \sigma$ in the vicinity of this limit, $\mathcal{B}_{\rm QR}$ is represented in the ϖ–σ plane by

$$B_{\rm QR}(\varpi, \sigma) \equiv \varpi^2 - 3^{2/3}\sigma^{4/3} + \sigma_0^2 = 0. \tag{30}$$

The sign of $B_{\rm QR}(\varpi, \sigma)$ tells whether the point ϖ–σ is in the NR domain ($B_{\rm QR} > 0$) or in the QR one ($B_{\rm QR} < 0$). The QR domain is then cut out of the $\varpi - \sigma$ domain, the remainder constituting the properly defined NR domain. The kernels of the integrands in equations (28) and (29) are kept at their NR values when in the NR domain. For perfect accuracy, the kernels in the QR region should be taken to be those in equations (99) and (100). When however the QR region does not contribute predominantly, these complicated kernels can be replaced by simple approximations. Their effect essentially being to limit the growth of the modulus of the NR kernels when the QR region is reached, we replace them by linear interpolations in ϖ, at fixed σ, between the values of the NR kernels evaluated on the border $\mathcal{B}_{\rm QR}$ for that value of σ. Let $\Theta_{\rm H}(y)$ denote the Heaviside function, equal to unity for positive argument y and zero otherwise. The above-described approximations to f and h can be written as

$$f_{\rm MF} = 2\pi s_q \frac{\omega_{\rm pr}^2\Omega^2}{c\,\omega^3}\iint \frac{m^3c^3}{\sin^2\alpha}\,{\rm d}\varpi\,{\rm d}\sigma\;\varpi\left[\Theta_{\rm H}^{+}\frac{x^2}{2\,(\sigma^2-x^2)^{3/2}} + \Theta_{\rm H}^{-}\frac{x_{\rm QR}^2}{2\,(\sigma^2-x_{\rm QR}^2)^{3/2}}\right]\frac{\partial F_0}{\partial\sigma}, \tag{31}$$

$$h_{\rm MF} = -\pi\frac{\omega_{\rm pr}^2\Omega^2}{c\,\omega^3}\iint \frac{m^3c^3}{\sin^2\alpha}\,{\rm d}\varpi\,{\rm d}\sigma\left[\Theta_{\rm H}^{+}\frac{2x^4(\sigma^2-x^2)+\sigma_0^2\,x^2(4\sigma^2+x^2)}{8\,(\sigma^2-x^2)^{7/2}} + \Theta_{\rm H}^{-}\frac{2x_{\rm QR}^4(\sigma^2-x_{\rm QR}^2)+\sigma_0^2\,x_{\rm QR}^2(4\sigma^2+x_{\rm QR}^2)}{8\,(\sigma^2-x_{\rm QR}^2)^{7/2}}\right]\frac{\partial F_0}{\partial\sigma}. \tag{32}$$

where $\Theta_{\rm H}^{\pm} = \Theta_{\rm H}(\pm B_{\rm QR}(\varpi,\sigma))$ and $\varpi_{\rm QR}(\sigma)$ and $x_{\rm QR}(\sigma)$ are the values of $|\varpi|$ and x on the boundary $\mathcal{B}_{\rm QR}$ for the given value of σ (equation 30). Equations (31) and (32) provide approximate values of the transfer coefficients f and h valid for isotropic as well as for non-isotropic distribution functions. The approximations in equations (31) and (32) will be illustrated in the example of a thermal distribution function in Section 3.2.4.

3.1.4 LF limit

When the reverse inequality to equation (27) applies in a strong sense, both the NR and QR domains contribute to the transfer coefficients. For a given frequency and a given propagation angle, α, this essentially happens when the dynamical variable σ of the particle is above the limit defined by equation (30) for $\varpi = 0$ or when its Lorentz factor γ largely exceeds the threshold defined by the reverse of inequality (27), which happens when the frequency ω is much less than the critical synchrotron frequency for a particle of Lorentz factor γ travelling in the direction of the considered radiation (equation 101). We refer to this situation as the LF limit. The LF contribution to the Faraday coefficients comprises both NR and QR parts, which we calculate for isotropic distributions in Sections 6.3 and 6.4.

3.2 Kernels of polarization transfer coefficients for isotropic distribution functions

Let us illustrate how to use equations (25) and (26) in isotropic models of the distribution function. When the distribution function is isotropic, it depends only on the Lorentz factor γ of the particles, but nevertheless depends on both variables ϖ and σ. When dealing with isotropic distribution functions, it is therefore wise to change from the variables ϖ, σ to the variables ϖ, γ. Integrating over ϖ, which then does not involve the distribution function, equations (25) and (26) can be written in the general form

$$f = \frac{\omega_{pr}^2\Omega^2}{c\,\omega^3}\,m^3c^3\int_1^\infty {\rm d}\gamma\,\frac{{\rm d}F_0}{{\rm d}\gamma}\,F^{\rm iso}(\gamma)\,, \qquad\qquad h = \frac{\omega_{pr}^2\Omega^2}{c\,\omega^3}\,m^3c^3\int_1^\infty {\rm d}\gamma\,\frac{{\rm d}F_0}{{\rm d}\gamma}\,H^{\rm iso}(\gamma), \tag{33}$$

where $F^{\rm iso}(\gamma)$ and $H^{\rm iso}(\gamma)$ are one-variable kernels for isotropic distribution functions.

3.2.1 Isotropic distributions in the HF limit

In the HF limit, the integration over ϖ in equations (28) and (29), which defines these kernels, extends, for a given value of γ, over the full domain. The kernels $F^{\rm iso}$ and $H^{\rm iso}$ can then be written in this case as

$$F_{\rm HF}^{\rm iso}(\gamma) = \frac{2\pi s_q}{\sin^2\alpha}\int_{\varpi_-}^{\varpi_+}{\rm d}\varpi\;\left(\frac{\varpi\,x^2}{2\,(\sigma^2-x^2)^{3/2}}\right). \tag{34}$$

$$H^{\rm iso}_{\rm HF}(\gamma) = -\frac{\pi}{\sin^2\alpha}\int_{\varpi_-}^{\varpi_+} {\rm d}\varpi \ \left(\frac{2x^4(\sigma^2-x^2)+\sigma_0^2\,x^2(4\sigma^2+x^2)}{8\,(\sigma^2-x^2)^{7/2}}\right). \tag{35}$$

The variables σ, x and (σ^2-x^2) can be expressed from equation (A2) in terms of γ, ϖ and parameters in equation (23) as

$$\sigma = \gamma\, u\sin^2\!\alpha + \varpi\,\cos\alpha\,, \qquad x^2 = (u^2(\gamma^2\sin^2\!\alpha-1)+2\gamma u\,\varpi\cos\alpha-\varpi^2)\sin^2\alpha\,, \qquad \sigma^2-x^2 = \varpi^2+u^2\sin^2\!\alpha. \tag{36}$$

The boundaries $\varpi_-(\gamma)$ and $\varpi_+(\gamma)$ of the integration over ϖ at a given γ are the abscissas of the intersection of the line of constant γ with the boundary of the physical domain in the ϖ–σ plane (Fig. A1). Since this boundary is where $x=0$, equation (36) implies that

$$\varpi_\pm(\gamma) = u\left(\gamma\cos\alpha \pm \sqrt{\gamma^2-1}\right). \tag{37}$$

The integration over ϖ in equations (34) and (35) plays the role of an angular integration. It can be performed analytically, the results, valid at HF, eventually being

$$F^{\rm iso}_{\rm HF}(\gamma) = 4\pi s_q\,\frac{\omega\cos\alpha}{|\Omega|}\left(\gamma\,\mathcal{L}(\gamma)-\sqrt{\gamma^2-1}\right), \qquad \text{where} \qquad \mathcal{L}(\gamma) = \cosh^{-1}\!(\gamma) = \ln\left(\sqrt{\gamma^2-1}+\gamma\right), \tag{38}$$

$$H^{\rm iso}_{\rm HF}(\gamma) = -\pi\,\frac{\sin^2\alpha}{2}\left(\gamma\,\sqrt{\gamma^2-1}\,\left(2\gamma^2-3\right)+\mathcal{L}(\gamma)\right). \tag{39}$$

3.2.2 Isotropic distributions in the LF limit

It comes out of the discussion in Section 5.4 that the coefficient of Faraday rotation f does not depart much from its NR approximation, although corrections are necessary for quantitative agreement in LF situations. We find in Section 6 that the isotropic kernel for f can be written in the LF limit as

$$F^{\rm iso}_{\rm LF}(\gamma) = \pi s_q\,\frac{\omega\cos\alpha}{|\Omega|}\,\gamma\left(\frac{4}{3}\,\ln\left(\frac{\gamma u}{\sin\alpha}\right)-1.260\,724\,39\right). \tag{40}$$

By contrast, the Faraday conversion coefficient h drastically differs from its HF expression when there is a QR contribution. The kernel of this coefficient is derived in Section 6.3 in the LF limit and for an isotropic distribution function. It can then be written as

$$H^{\rm iso}_{\rm LF}(\gamma) = \frac{\pi}{8}\left(\frac{\omega^2\sin\alpha}{\Omega^2}\right)^{2/3}\left(4-\frac{1}{3^{4/3}}\right)\,\gamma^{4/3}. \tag{41}$$

3.2.3 Exact isotropic kernels and composite approximations to them

The results in Sections 3.2.1 and 3.2.2 apply in different regions of the energy space. For distributions with only a very few particles in the LF regime, the HF approximation is sufficient. When the distribution is more extended in energy than the threshold $\gamma_{\rm QR}$ defined in equation (98), the kernels should account for the QR contribution in the LF regime. They may then be calculated by integrating over ϖ at fixed γ the right-hand sides of equations (25) and (26). This however requires a double numerical integration. Section 6.5 proposes an approximate formula interpolating between the HF expression of these kernels, valid when $\gamma < \gamma_{\rm QR}$, and their asymptotic LF expressions, valid for $\gamma \gg \gamma_{\rm QR}$. Huang & Shcherbakov (2011) adopt a similar approach by providing fits to their numerically computed kernels and claim similar accuracy.

For extended energy distributions, the region at $\gamma \sim \gamma_{\rm QR}$ should not dominantly contribute to integrals such as those in equation (33). These interpolation formulae then provide about 10 per cent accuracy on h for power-law distributions and slightly better accuracy on f. When on the contrary the energy range close to $\gamma_{\rm QR}$ is determinant, the MF approximations in equations (31) and (32) could be used instead or, if accurate results are needed, the transfer coefficients would be numerically calculated from equations (25) and (26) by double integrating over the variables ϖ and σ.

3.2.4 Illustrations and comparison to known results

Previous approaches to polarization transfer coefficients. The polarization transfer coefficients for a thermal distribution have been previously derived exactly, by a method entirely different from ours, in a form that eventually requires only one numerical quadrature (Trubnikov 1958). It is therefore of interest to test different approximate results against this exact result, or against results proposed for the thermal case by different authors. Trubnikov (1958) considers a Jüttner distribution, as in equation (42) below. The conductivity is derived by integrating the changes of the perturbed distribution function over the delay time along unperturbed trajectories, just as shown in Section 2, and then taking suitable moments of the components of momentum. The exponential dependence of the Jüttner distribution on energy can be associated with the complex exponential that arises from the evolution over time of the phase functions, as in equation (57). The integration over the particle's energy can then be carried out, yielding a result that involves a modified Bessel function of the second kind of a complex argument

depending on the delay time (Melrose 1997a; Shcherbakov & Huang 2011). The integration over the delay time then remains to be carried out. This can be done by different numerical strategies (Huang & Shcherbakov 2011; Shcherbakov & Huang 2011), yielding exact results. Else, it can be carried out analytically in an approximate way in different limits (Melrose 1997c; Shcherbakov 2008) or by using the method of stationary phase (Melrose 1997d). Swanson (2002) calculates the dielectric tensor of a moderately relativistic thermal plasma from the familiar multiple resonance series (Bekefi 1966) which he sums in a form similar to our equation (65) below, yielding expressions that involve Bessel functions depending on a continuous argument. This approach is analogous to those used by Qin, Phillips & Davidson (2007), Heyvaerts (1970), Thiébaut (2010) and in this paper, where we furthermore take full advantage of the high harmonic limit. Swanson (2002) then uses his result to perform the integration over the directions of motion of the particles in terms of hypergeometric functions for which he presents approximations suitable for weakly relativistic plasmas. Huang & Shcherbakov (2011) have extended Trubnikov's approach to non-thermal isotropic distribution functions, the integration with respect to delay time being performed first for a given value of the Lorentz factor. These authors numerically calculate transfer coefficients for Dirac distributions in energy and provide fitting formulae for the kernels of Faraday rotation and conversion. The coefficients for arbitrary isotropic distributions may be obtained by a further integration over energy. Examples are provided for power-law distributions covering a finite energy interval and for thermal distributions. In the following sections we compare our results for a thermal distribution to results obtained by these approaches.

Polarization transfer coefficients for a thermal distribution in the HF limit. Following Shcherbakov (2008) we express the thermal Jüttner distribution as

$$F_0(\gamma) = \frac{\exp(-\gamma/T)}{4\pi m^3 c^3 T K_2\left(T^{-1}\right)}, \quad \text{normalized so that} \quad \int 4\pi\gamma\sqrt{\gamma^2-1}\, m^3c^3 F_0(\gamma)\,\mathrm{d}\gamma = 1, \tag{42}$$

where T is the ratio of the thermal energy to the rest-mass energy of the particles. By Trubnikov's method, Shcherbakov (2008) finds the following polarization transfer coefficients in the HF limit

$$f^{\rm th}_{\rm HF} = \frac{\Omega\cos\alpha\,\omega_{\rm pr}^2 K_0\left(T^{-1}\right)}{c\,\omega^2 K_2\left(T^{-1}\right)}, \qquad \text{and} \qquad h^{\rm th}_{\rm HF} = \frac{\Omega^2\sin^2\!\alpha\,\omega_{\rm pr}^2\left(K_1\left(T^{-1}\right)+6T\,K_2\left(T^{-1}\right)\right)}{2c\omega^3 K_2\left(T^{-1}\right)}, \tag{43}$$

where K_1 and K_2 are modified Bessel functions of the second kind. In this HF limit his results are identical to ours. To compare them, we evaluate f and h from equations (38) and (39), also valid in this limit, considering the case of an electronic population, so that $s_q = -1$. The f coefficient, derived from equations (33) and (38), becomes in this case

$$f^{\rm th}_{\rm HF} = \frac{\Omega\,\cos\alpha\,\omega_{\rm pr}^2}{c\,\omega^2}\frac{1}{T^2 K_2\left(T^{-1}\right)}\int_1^\infty \mathrm{d}\gamma\;\mathrm{e}^{-\gamma/T}\left(\gamma\,\mathcal{L}(\gamma)-\sqrt{\gamma^2-1}\right). \tag{44}$$

Keeping the integrand part in $\sqrt{\gamma^2-1}$ untouched, the term $\gamma\,\mathcal{L}(\gamma)\exp(-\gamma/T)$ is integrated by parts, giving successively

$$\int_1^\infty \mathrm{d}\gamma\;\gamma\;\mathcal{L}(\gamma)\,\mathrm{e}^{-\gamma/T} = T^2\int_1^\infty \mathrm{d}\gamma\;\frac{\mathrm{e}^{-\gamma/T}}{\sqrt{\gamma^2-1}} + T\int_1^\infty \mathrm{d}\gamma\;\frac{\gamma}{\sqrt{\gamma^2-1}}\,\mathrm{e}^{-\gamma/T} = T^2\,K_0(T^{-1}) + \int_1^\infty \mathrm{d}\gamma\;\sqrt{\gamma^2-1}\,\mathrm{e}^{-\gamma/T}, \tag{45}$$

where the last equality has been obtained again by integrating by parts the second integral of the middle part. Substituting this into equation (44), we recover $f^{\rm th}$ in equation (43). Starting from equations (33) and (39) for $h^{\rm iso}_{\rm HF}$ we similarly recover $h^{\rm th}_{\rm HF}$ in equation (43) by noting that $\int \mathrm{d}\gamma\;\mathcal{L}(\gamma)\exp(-\gamma/T) = T\,K_0(T^{-1})$ and that

$$\int_1^\infty \mathrm{d}\gamma\;\gamma\,(2\gamma^2-3)\sqrt{\gamma^2-1}\,\mathrm{e}^{-\gamma/T} = T\,\left(-K_2(T^{-1})+6\,T\,K_3(T^{-1})\right) = -T\,K_0(T^{-1}) + 4T^2\left(K_1(T^{-1})+6\,T\,K_2(T^{-1})\right). \tag{46}$$

Polarization transfer coefficients for a thermal distribution in the MF regime. Stepping out of the domain of validity of the HF approximation, Fig. 1 comparatively illustrates the behaviour of different approximations to the polarization coefficients by representing their HF approximations (43) and contrasting them to the numerical estimation of their exact counterparts (equations 25 and 26) and to the fits provided by Shcherbakov (2008) to describe this regime. The difference between the approximations to $f^{\rm th}$ being small, the left-hand panel of Fig. 1 represents their ratio to their HF approximation. These ratios are displayed as a function of the parameter

$$X = T\left(10^3\sqrt{2}\,\sin\alpha/u\right)^{1/2}, \tag{47}$$

defined in Shcherbakov (2008), which is proportional to the square root of the left-hand side of the inequality in equation (27). The right-hand panel of Fig. 1 shows the corresponding approximations to $h^{\rm th}$ as a function of temperature, the quantity represented in this case being the coefficient itself. This figure uses the following fiducial parameters $m = c = 1$, $\alpha = \pi/4$, $u = 15$. It is found that the region-cut approximation to the intermediate regime discussed in Section 3.1 and represented by the expressions in equations (31) and (32) provides a good extension of these coefficients to higher temperatures where the HF limit becomes insufficient.

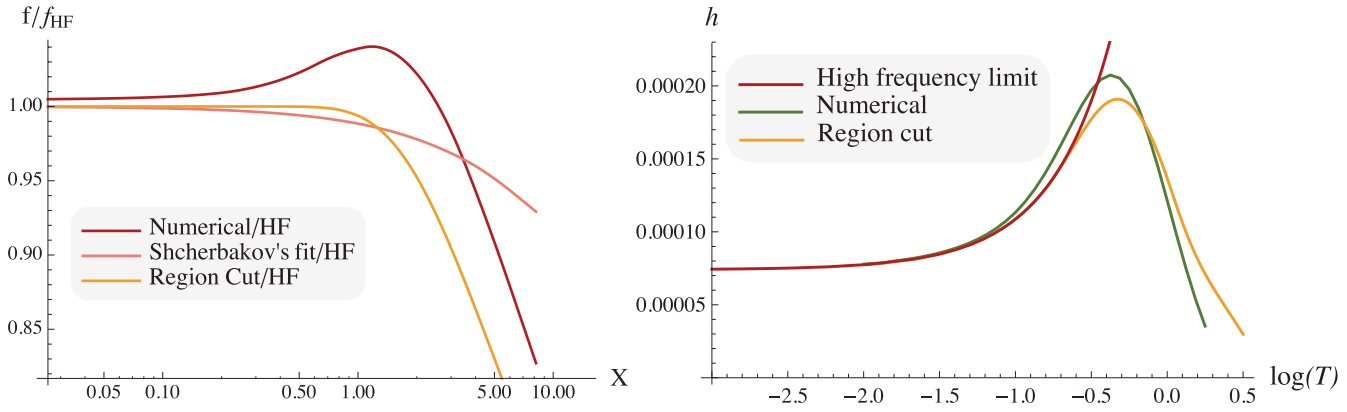

Figure 1. Left: ratio to the HF expression $f_{\rm HF}^{\rm th}$ in equation (43) of, respectively, the numerically computed value of the thermal Faraday rotation coefficient $f^{\rm th}$ for the isothermal model of equation (42), based on equation (25), the fit formula provided for it by Shcherbakov (2008) and the region-cut approximation in equation (31), as labelled. These ratios are displayed as a function of the scaling parameter X introduced by Shcherbakov (2008), defined in equation (47). Right: the HF limit of the Faraday conversion coefficient $h^{\rm th}$ from equation (43), the region-cut formula from equation (32) and the almost exact value numerically computed from equation (25), as a function of the temperature, T (as labelled). In both cases, the region-cut procedure around the resonant particles seems to improve significantly the domain of validity of the match to the exact transfer coefficients.

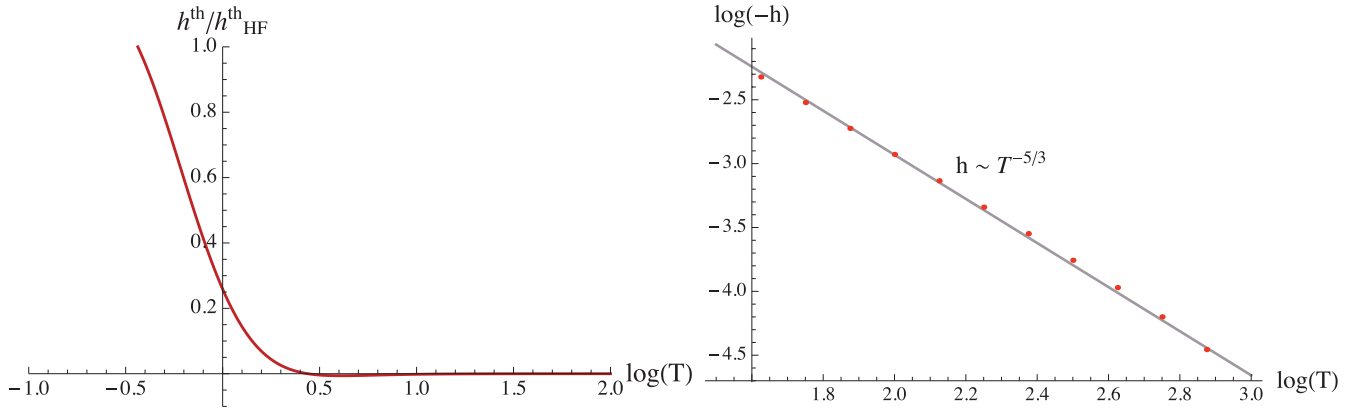

Figure 2. Left: the evolution with temperature T of the ratio of $h^{\rm th}$ to its HF approximation $h_{\rm HF}^{\rm th}$. Right: the evolution of $\log|h|$ versus $\log T$. The $T^{-5/3}$ asymptote at large T is a direct consequence of the $\gamma^{4/3}$ asymptotic behaviour of the isotropic kernel of the Faraday coefficient h at large γ.

Polarization transfer coefficients for a thermal distribution in the LF limit. As an illustration of equation (41) let us consider again the isothermal distribution, equation (42). It follows that when most particles interact with the radiation in the LF regime we expect

$$h_{\rm LF}^{\rm th} \propto -\frac{1}{8\pi}\left(\frac{1}{T}\right)^{5/3}\Gamma\left(\frac{7}{3}\right), \tag{48}$$

which corresponds indeed to the asymptotic behaviour that can be computed numerically (using the Olver uniform expansion; see Section 6.2 and Appendix G), as shown in Fig. 2.

Polarization transfer coefficients for an isotropic power-law distribution function. Let us also consider a power-law distribution scaling like γ^{-n} with a low-energy cutoff $\gamma_{\rm m}$, such as

$$F_0(\gamma) = \frac{\Theta_{\rm H}(\gamma-\gamma_{\rm m})}{N(\gamma_{\rm m},n)\,\gamma^n}. \tag{49}$$

For an isotropic distribution, assuming $n > 3$ for convergence, the normalization factor $N(\gamma_{\rm m}, n)$ results from equation (42)

$$\frac{4\pi m^3c^3}{N(\gamma_{\rm m},n)}\int_{\gamma_{\rm m}}^{\infty}\frac{\sqrt{\gamma^2-1}\,\gamma\,{\rm d}\gamma}{\gamma^n} = 1. \tag{50}$$

The Faraday coefficients can be expressed for such distribution functions in terms of a γ-dependent kernel as in equation (33). The low-energy cutoff introduces a Dirac-type singularity in the derivative ${\rm d}F_0/{\rm d}\gamma$ at $\gamma_{\rm m}$, that should be taken care of when equation (33) is used. Alternatively, these relations may be integrated by parts, the integrated term vanishing because F_0 vanishes at infinity and the kernels do at $\gamma = 1$.

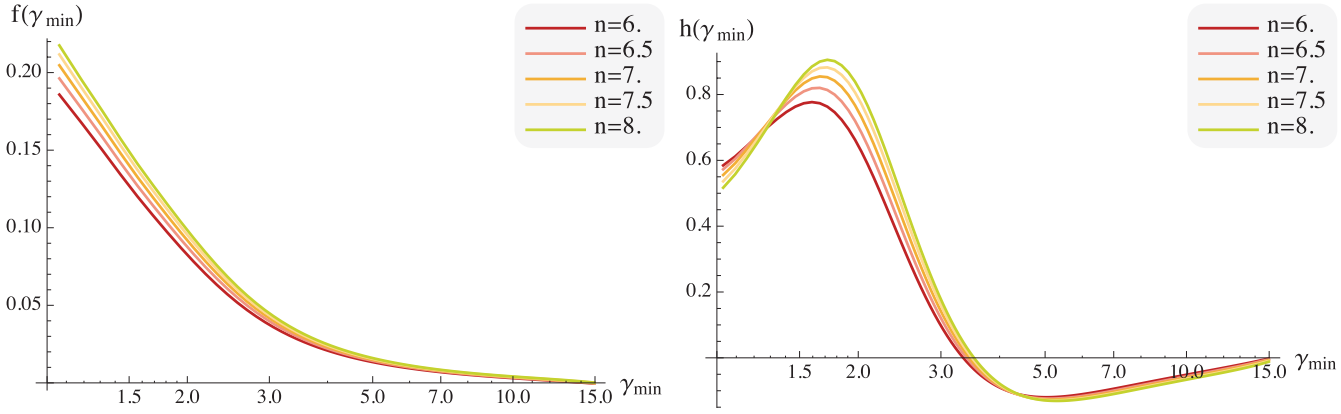

Figure 3. Polarization transfer coefficients (left: $f_{\rm iso}^{\rm pl}$ and right: $h_{\rm iso}^{\rm pl}$) for an isotropic power-law distribution function as a function of the low-energy cutoff $\gamma_{\rm min}$ for different values of the power-law index n, as labelled. The coefficient f is normalized to $-\pi s_q \cos\alpha(\omega_{\rm pr}^2\,|\Omega|\,/c\omega^2)$ and h to $\omega_{\rm pr}^2\Omega^2/c\omega^3$. This figure has been produced by numerically integrating equations (25) and (26) over ϖ and σ for the distribution (49).

Fig. 3 shows the polarization transfer coefficients for power-law distributions of various exponents as a function of the low-energy cutoff $\gamma_{\rm min}$. These coefficients have been numerically calculated from equations (25) and (26) by integrating over ϖ and σ for the distribution (49), using equation (A1) to express γ in terms of σ and ϖ.

Approximations to the one-variable kernels could have been used instead. We derive in Section 6.5 approximations to $F^{\rm iso}(\gamma)$ and $H^{\rm iso}(\gamma)$ obtained by interpolating between their HF expressions and their asymptotic LF limits. They provide results of reasonable, though limited, accuracy, but conveniently reduce the calculation to a simple one-variable quadrature. Fig. L1 in Appendix L compares the results in Fig. 3 with those obtained from these approximations. Equations (33), (50) and (40) indicate that $f^{\rm pl}$ scales for large $\gamma_{\rm m}$ as $\ln(\gamma_{\rm m})/\gamma_{\rm m}^2$.

In a distribution that is extended in energy, particles of Lorentz factor γ less than the upper limit $\gamma_{\rm QR}$ defined by equation (27) contribute in the HF regime, as in equations (38) and (39), while particles of a larger Lorentz factor bring a QR contribution that should be added to their NR one. For $\gamma \gg \gamma_{\rm QR}$, these two contributions add to form the asymptotic LF contribution to the coefficients in equations (40) and (41). The QR contribution to the coefficient f is small but does not vanish, being the integral of an almost odd function over an interval almost symmetrical with respect to zero (Appendix J). The isotropic LF kernel that results for f is derived in Section 6 and is shown in equation (130).

3.3 Polarization transfer coefficients for anisotropic distribution functions

The HF results in equations (28) and (29) make no assumption about the isotropy, or otherwise, of the distribution function F_0. But for the work of Melrose (1997b) on anisotropic thermal plasmas, there does not seem to be any other result published so far in the literature on general anisotropic distributions. Huang & Shcherbakov (2011) give results and fits for a number of isotropic distribution functions, including monoenergetic ones. The form in which our results are obtained allows us to calculate transfer coefficients in the HF approximation not only for isotropic distribution functions but also for a large class of anisotropic ones, providing the first terms of an expansion of the anisotropy in multipoles. Strong anisotropies still demand a two-variable quadrature, as exemplified by the beam model below. Stepping out of the HF limit in this case would provide one-variable quadratures that are no simpler than the two-variable ones from which they originate. We therefore restrict ourselves in this section to HF results for different anisotropic distribution functions.

3.3.1 Quadrupolar and higher multipolar anisotropies at HF

Let us parametrize quadrupolar anisotropic distribution functions as the product of a function of the Lorentz factor γ of the particles and a second-order Legendre function of the cosine of the particle's pitch angle ϑ, defined such that $p_\parallel = p\cos\vartheta$:

$$F(\gamma,\vartheta) = F_2(\gamma)P_2(\cos\vartheta). \tag{51}$$

For such distributions it is best to switch to the spherical coordinates γ and ϑ. The σ and ϖ derivatives of the distribution function in equations (25) and (26) or in equations (28) and (29) always separate into the sum of two terms, one of which is proportional to $\mathrm{d}F_2/\mathrm{d}\gamma$ and the other is proportional to F_2. Generically, owing to the factorization property of the distribution function as in equation (51), the transfer coefficient could be written, for example in the case of the Faraday rotation coefficient f, as

$$f_{\rm HF}^{\rm aniso} = A_f \int_1^\infty \gamma\,\mathrm{d}\gamma\,\left(\frac{\mathrm{d}F_2}{\mathrm{d}\gamma}\,D'_f(\gamma,\mu) + F_2(\gamma)D_f(\gamma,\mu)\right), \tag{52}$$

where A_f is a constant factor, still dependent on ω and α, and the functions, respectively, multiplying $F_2'(\gamma)$ and $F_2(\gamma)$, $D_f'(\gamma, \mu)$ and $D_f(\gamma, \mu)$, depend on γ and on the parameter $\mu = \cos\alpha$, α being the propagation angle of the radiation (Fig. 5). Similar quantities referring to the coefficient h can be defined. From equations (28) and (29), using equations (36) and (A1), it follows after integration over ϑ that, for the quadrupolar model in equation (51)

$$f_{\rm HF}^{\rm aniso} = \pi s_q \frac{\omega_{\rm pr}^2\,|\Omega|}{c\,\omega^2} m^3c^3 \int \gamma\,{\rm d}\gamma \frac{{\rm d}F_2}{{\rm d}\gamma} \left(\frac{4\mathcal{L}(\gamma)\left(3\left(2\gamma^2+3\right)P_3(\mu) - \left(\gamma^2-1\right)\mu\right)}{5\left(\gamma^2-1\right)} + \frac{4\left(\left(\gamma^2-1\right)\mu - \left(11\gamma^2+4\right)P_3(\mu)\right)}{5\gamma\left(\gamma^2-1\right)^{1/2}} \right)$$
$$+ \pi s_q \frac{\omega_{\rm pr}^2\,|\Omega|}{c\,\omega^2} m^3c^3 \int \gamma\,{\rm d}\gamma\, F_2(\gamma) \left(\frac{6\mathcal{L}(\gamma)\left(2\left(\gamma^4-1\right)\mu - \left(2\gamma^4+15\gamma^2+3\right)P_3(\mu)\right)}{5\gamma\left(\gamma^2-1\right)^2} + \frac{\left(34\gamma^2+86\right)P_3(\mu) - 24\left(\gamma^2-1\right)\mu}{5\left(\gamma^2-1\right)^{3/2}} \right), \tag{53}$$

and

$$h_{\rm HF}^{\rm aniso} = \pi \frac{\omega_{\rm pr}^2\Omega^2}{c\,\omega^3} m^3c^3 \int \gamma\,{\rm d}\gamma\, F_2(\gamma) \left(\frac{\mathcal{L}(\gamma)\left(\left(24\gamma^2+5\right)P_2(\mu) - 12\left(2\gamma^2+1\right)P_4(\mu) + 7\right)}{7\left(\gamma^2-1\right)^2} \right.$$
$$\left. - \frac{7\left(-6\gamma^4+17\gamma^2+4\right) + 5\left(18\gamma^4+65\gamma^2+4\right)P_2(\mu) - 12\left(4\gamma^4+37\gamma^2+4\right)P_4(\mu)}{105\gamma\left(\gamma^2-1\right)^{3/2}} \right)$$
$$+ \pi \frac{\omega_{\rm pr}^2\Omega^2}{c\,\omega^3} m^3c^3 \int \gamma\,{\rm d}\gamma \frac{{\rm d}F_2}{{\rm d}\gamma} \left(\frac{\mathcal{L}(\gamma)\left(14\gamma^2 - 108\gamma^2 P_4(\mu) + \left(94\gamma^2-7\right)P_2(\mu) + 7\right)}{42\gamma\left(\gamma^2-1\right)} \right.$$
$$\left. + \frac{7\left(4\gamma^4-8\gamma^2+19\right) + 5\left(-20\gamma^4+76\gamma^2+31\right)P_2(\mu) + 36\left(2\gamma^4-9\gamma^2-8\right)P_4(\mu)}{210\left(\gamma^2-1\right)^{1/2}} \right). \tag{54}$$

Equations (53) and (54) are analytical expressions, valid in the HF limit, for the Faraday coefficients f and h for an anisotropic distribution function of the form (51). Appendix I gives the corresponding coefficients D_f' and D_f for higher multipoles of the form $F_n(\gamma)P_n(\mu)$ for $n = 0, 1, \ldots, 6$. Any axisymmetric distribution $F(\gamma, \vartheta)$ can be represented as a linear combination of such functions, as $F(\gamma, \vartheta) = \sum_n F_n(\gamma)P_n(\cos\vartheta)$. Since the conductivity depends linearly on the unperturbed distribution function, the conductivity of a sum of functions is the sum of the corresponding conductivities. In each individual term, neither the multipole 'distribution function' $F_n(\gamma)$ nor the angular factor $P_n(\cos\vartheta)$ needs to be positive. The only constraint is that the sum over n be positive for any γ and ϑ.

As expected, the coefficients f and h depend on the direction of propagation α in a different manner than those associated with an isotropic distribution function given in equations (38) and (39). For a quadrupolar distribution, f varies with α as a combination of $P_1(\cos\alpha)$ and $P_3(\cos\alpha)$ while h varies as a combination of $P_2(\cos\alpha)$ and $P_4(\cos\alpha)$.

3.3.2 Beam model at HF

Let us consider now an anisotropic distribution representing a beam. Since theory is constructed for particles, the unperturbed motion of which is ruled only by the static magnetic field in the chosen frame of reference, the beam must be assumed to propagate parallel to the magnetic field. Otherwise, for example for winds propagating at an angle to the magnetic field, a static convection electric field would also be present in the observer's frame and the calculation in Section 2.2 would then have to be revisited or the Stokes parameters transformed from the beam proper frame to the observer's frame. We form the beam distribution $F_\star$ by boosting an isothermal distribution, so that

$$F_\star(\gamma, \theta) \propto \exp\left(-\gamma_\star(p, \theta)/T\right), \quad \text{where } \gamma_\star(p, \theta) \text{ obeys } \quad c^2m^2\gamma_\star^2(p, \vartheta) = c^2m^2 + \left(p_\star + p\cos(\vartheta)\right)^2 + p^2\sin^2(\vartheta). \tag{55}$$

For such a distribution, the derivative of $F_\star$ with respect to σ entering equations (28) and (29) is given by

$$\frac{\partial F_\star}{\partial\sigma} = -F_\star \frac{|\,\Omega\,|}{T\,\omega\,\gamma_\star\sin^2\alpha} \left(\sqrt{c^2m^2+p^2} + \cos(\alpha)\,p_\star\right). \tag{56}$$

For the purpose of numerical integration, equations (28), (29) and (56) are expressed as a function of $p_\perp$ and $p_\parallel$. The result of this integration, valid in the HF limit, is shown in Fig. 4 for our beam model and for different values of $p_\star$ and T as labelled, with the same fiducial parameters as above. As expected, for $p_\star = 0$ we recover the thermal solution of Section 3.2.4, but as the beam becomes more anisotropic (i.e. $p_\star$ increases at fixed T, or T decreases at fixed $p_\star \neq 0$), the Faraday coefficients are more focused near the axis of symmetry. This may be understood from the fact that the values of the kernels depending on ϖ and σ in equations (28) and (29) are the largest where the difference $\sigma^2 - x^2$ is the smallest, that is where the pitch angle ϑ of the particle is closest to the direction of propagation α of the radiation, causing a larger response when the angle α is in the particle's beam.

The next two sections formally carry out two of the four integrals involved in equation (24) in order to write equations (25) and (26), and investigate the corresponding resonant and non-resonant regimes. A detailed analysis of the various frequency regimes allows us to write simple one-dimensional quadrature. These two sections can be skipped on a first read.

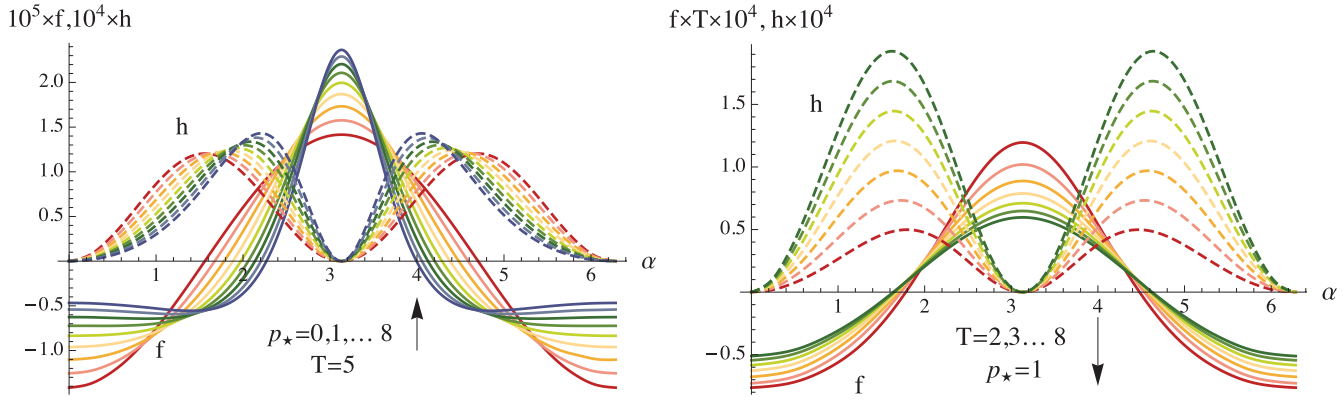

Figure 4. Polarization transfer coefficients (f, h) versus the angle of propagation α, represented here on the interval $[0,\ 2\pi]$ for the 'beam' model of Section 3.3.2 as a function of the beam momentum parameter $p_\star$ (left-hand panel) and the temperature T (right-hand panel), as labelled. The vertical arrows indicate in which sense the parameter varies at $\alpha = \pi$. The Faraday response becomes more collimated along the magnetic field direction as the distribution becomes more anisotropic or colder.

4 DERIVATION OF THE POLARIZATION TRANSFER COEFFICIENTS

We now describe our derivation of the polarization transfer coefficients, which amounts to calculating the elements of the Hermitian and anti-Hermitian parts of the conductivity deduced from equation (24), that is, of the phase integrals in equation (22). The usual approach to the phase integrals is to integrate over the time delay τ by expanding $\exp(\mathrm{i}x\sin\phi)$, or any similar expression, in a discrete Fourier series such as for example $\exp(\mathrm{i}x\sin\phi) = \sum_n J_n(x)\ \exp(\mathrm{i}\,n\,\phi)$, where $J_n(x)$ is a Bessel function of relative integer order. An integration over times t' earlier than t (that is over positive delay times $\tau = t - t'$) is then performed that yields resonant denominators $\omega - k_\parallel v_\parallel - n\Omega_*$. The integrand being proportional to $\exp(+\mathrm{i}\omega\tau)$, and it being understood that ω really is a complex Laplace variable, the resonant denominators should be regarded as having an infinitesimal positive imaginary part, ensuring the convergence of integrals over τ at $\tau = +\infty$. These denominators are then to be understood as complex numbers with an infinitesimal positive imaginary part, the real part of which is the Cauchy principal value, the imaginary part being $-\mathrm{i}\pi\delta_{\mathrm{D}}(\omega - k_\parallel v_\parallel - n\Omega_*)$. This gives an exact expression of the conductivity (Bekefi 1966) in the form of a series, each term of which involves one such resonant denominator.

However, since any approximation to the sum of these series has, in the present context, to be carried out up to very large values of n, of order $\omega/|\Omega_*|$ at least, this representation of the conductivity is not suitable for our purpose. As when deriving the synchrotron emission spectrum, it would be preferable to somehow substitute to the discrete series a representation in which the discrete summation is replaced by an integration over a continuous variable. Sazonov (1969b) attempted this by changing the discrete sums into integrals, considering the index n of the Bessel functions as being a continuous variable which can be identified with the variable σ defined in equation (23). This approach is known to be successful when evaluating the dissipative part of the conductivity, in which the many resonant Dirac functions form a sum similar to a Riemann one that can be approached by the integral of the so-defined interpolating function, $F(\sigma)$ say. But this is an unfortunate approach for calculating the non-dissipative part, in which principal values are involved. A continuous approximation to the derivative of $F(\sigma)$ would have been preferable in this case, although any a priori choice of such an interpolation would be tainted with arbitrariness.

4.1 An exact continuous-spectrum-type representation of the conductivity

We improve here over Sazonov's approach by deriving exact expressions for the phase integrals in equation (22) as functions of the continuous variable σ defined in equation (23). This variable will eventually appear as a continuous index of some Bessel functions. This will achieve, without any arbitrariness, the desired continuous-spectrum-type representation. Qin et al. (2007) have derived this transformation by using the invariance associated with the periodicity of the unperturbed motion while Heyvaerts (1970) and Thiébaut (2010) derived it by exactly turning the familiar discrete series representation into a continuous one by means of an integral representation of the principal values involved in the series. To show here how this is achieved, we follow a method similar to that of Qin et al. (2007). The phase integrals in equation (22) are first expressed in terms of the variables in equation (23) and the delay time τ is replaced by a delay angle ψ, so that

$$P_\varepsilon(\sigma,x,\phi) = \exp(-\mathrm{i}\,s_q(\sigma\phi - x\sin\phi))\int_{s_q\phi}^{+\infty}\frac{\mathrm{d}\psi}{|\Omega_*|}\ \exp(\mathrm{i}\,((\sigma+s_q\varepsilon)\,\psi - x\ \sin\psi))\,,\qquad \text{with}\qquad \psi = s_q\phi + |\Omega_*|\tau. \tag{57}$$

To account for the periodicity of the unperturbed motion, the integration range over the angle ψ is separated into segments of length 2π, and the integration on the nth segment is carried out by changing from ψ to $w = \psi - (s_q\phi + 2n\pi)$. Then,

$$P_\varepsilon(\sigma,x,\phi) = \frac{\exp(\mathrm{i}\,(\varepsilon\phi + s_q x\sin\phi))}{|\Omega_*|}\left(\sum_{n=0}^{\infty}\mathrm{e}^{2\mathrm{i}\pi n\,(\sigma+s_q\varepsilon)}\right)\int_0^{2\pi}\mathrm{d}w\ \exp(\mathrm{i}((\sigma+s_q\varepsilon)w - x\ \sin(w+s_q\phi))). \tag{58}$$

The fact that the periodicity of the motion is fully taken into account in this exact transformation could be considered superfluous because, on one hand, the period is very long in the ultrarelativistic limit and, on the other hand, the integral over ψ in equation (57) could conceivably be evaluated by the method of stationary phase applied to a unique interval of quasi-stationarity. It will however become clear below that the anti-Hermitian part of the conductivity is in fact not determined only by the properties of the motion near the quasi-stationary phase, a situation that may be compared to that of a classical plasma, in which the cyclotron resonances determine the rates of emission and absorption but where NR particles make the most of the contribution to the medium's dispersive properties. From equation (58) we calculate the combinations of the phase integrals that appear in equation (24), namely

$$\begin{pmatrix} P_0 \\ (P_+ - P_-)/\,2\mathrm{i} \\ (P_+ + P_-)/\,2 \end{pmatrix} = \frac{\mathrm{e}^{\mathrm{i}s_q x \sin\phi}}{|\,\Omega_*\,|} \left(\sum_{n=0}^{\infty} \mathrm{e}^{2\mathrm{i}\pi n\sigma}\right) \int_0^{2\pi} \mathrm{d}w\, \mathrm{e}^{\mathrm{i}(\sigma w - x\sin(w+s_q\phi))} \begin{pmatrix} 1 \\ \sin(\phi + s_q w) \\ \cos(\phi + s_q w) \end{pmatrix}. \tag{59}$$

The sum over n of the imaginary exponentials is not absolutely convergent. It should be regarded as a distribution rather than as a proper function because it enters an integration over the variable σ that will have to be performed at a later stage. We define three functions T_1, T_2, T_3 by

$$T_1 = 1\,, \qquad T_2 = \sin, \qquad T_3 = \cos\,. \tag{60}$$

The expressions in equation (59) are then inserted in equation (24) which gives the components of the current. Then gathering the terms which depend on the gyration angle ϕ and integrating over it, the components of the conductivity tensor can be written as

$$\sigma_{ij} = -\frac{2\pi q^2}{\omega} \int_{-\infty}^{+\infty} \mathrm{d}p_\parallel \int_0^{\infty} p_\perp \mathrm{d}p_\perp \; M_{ij}(p_\perp, p_\parallel, k_\perp, k_\parallel), \tag{61}$$

where the matrix M_{ij} is, with i a line index and j a column one:

$$\begin{pmatrix} v_\perp(\omega\frac{\partial f_0}{\partial p_\perp} + k_\parallel D(f_0))\, Q_{33}(\sigma,x) & v_\perp(\omega\frac{\partial f_0}{\partial p_\perp} + k_\parallel D(f_0))\, Q_{32}(\sigma,x) & (v_\perp\omega\frac{\partial f_0}{\partial p_\parallel}\, Q_{31}(\sigma,x) - k_\perp v_\perp D(f_0)\, Q_{33}(\sigma,x)) \\ v_\perp(\omega\frac{\partial f_0}{\partial p_\perp} + k_\parallel D(f_0))\, Q_{23}(\sigma,x) & v_\perp(\omega\frac{\partial f_0}{\partial p_\perp} + k_\parallel D(f_0))\, Q_{22}(\sigma,x) & (v_\perp\omega\frac{\partial f_0}{\partial p_\parallel}\, Q_{21}(\sigma,x) - k_\perp v_\perp D(f_0)\, Q_{23}(\sigma,x)) \\ v_\parallel(\omega\frac{\partial f_0}{\partial p_\perp} + k_\parallel D(f_0))\, Q_{13}(\sigma,x) & v_\parallel(\omega\frac{\partial f_0}{\partial p_\perp} + k_\parallel D(f_0))\, Q_{12}(\sigma,x) & (v_\parallel\omega\frac{\partial f_0}{\partial p_\parallel}\, Q_{11}(\sigma,x) - k_\perp v_\parallel D(f_0)\, Q_{13}(\sigma,x)) \end{pmatrix}. \tag{62}$$

The coefficients Q_{ab} that appear in equation (62), a and b varying between 1 and 3, encompass the results of the integrations over the delay angle and over the gyration angle. They depend on the sign s_q of the electric charge of the particle species and may eventually be written as

$$Q_{ab}(\sigma,x) = (-s_q)^{a+b} \left(2\pi\sum_{n=0}^{\infty} \mathrm{e}^{2\mathrm{i}\pi n\sigma}\right) G_{ab}(\sigma,x)\,, \quad \text{with} \quad G_{ab} = \int_0^{2\pi} \frac{\mathrm{d}\phi}{2\pi} \int_0^{2\pi} \frac{\mathrm{d}w}{2\pi}\, T_a(\phi) T_b(\phi - w) \mathrm{e}^{\mathrm{i}(\sigma w + x(\sin(\phi - w) - \sin\phi))}. \tag{63}$$

The parentheses in the first part of equation (63) can be more explicitly written as

$$2\pi\sum_{n=0}^{\infty} \mathrm{e}^{2\mathrm{i}\pi n\sigma} = \mathrm{i}\pi\, \frac{\mathrm{e}^{-\mathrm{i}\pi\sigma}}{\sin\sigma\pi} \left(\lim_{N\to\infty} \left(1 - \mathrm{e}^{2\mathrm{i}\pi N\sigma}\right)\right). \tag{64}$$

The calculation of the elements G_{ab} involves integrations over the angles ϕ and w. Qin et al. (2007) perform these integrations along the lines described in Appendix B. The elements G_{ab} may finally be expressed in terms of Bessel functions of the first kind, with indices σ or $-\sigma$ and argument x, as listed below:

$$G_{11}(\sigma,x) = \mathrm{e}^{\mathrm{i}\sigma\pi} J_\sigma(x) J_{-\sigma}(x) \qquad G_{12}(\sigma,x) = -\frac{\mathrm{i}}{2}\, \mathrm{e}^{\mathrm{i}\sigma\pi} \frac{\partial}{\partial x}(J_\sigma(x) J_{-\sigma}(x))\,,$$

$$G_{13}(\sigma,x) = \mathrm{e}^{\mathrm{i}\sigma\pi} \left(-\frac{\sin\sigma\pi}{\pi x} + \frac{\sigma}{x}\, J_\sigma(x) J_{-\sigma}(x)\right) \qquad G_{22}(\sigma,x) = \frac{\sin\sigma\pi}{\pi}\, \mathrm{e}^{\mathrm{i}\sigma\pi} \left(\frac{\pi}{\sin\sigma\pi}\, J'_\sigma(x) J'_{-\sigma}(x) + \frac{\sigma}{x^2}\right),$$

$$G_{23}(\sigma,x) = \frac{\mathrm{i}\sigma}{2x}\, \mathrm{e}^{\mathrm{i}\sigma\pi} \frac{\partial}{\partial x}(J_\sigma(x) J_{-\sigma}(x))\,, \qquad G_{33}(\sigma,x) = -\frac{\sigma}{\pi x^2}\, \sin\sigma\pi\, \mathrm{e}^{\mathrm{i}\sigma\pi} \left(1 - \frac{\pi\sigma}{\sin\sigma\pi}\, J_\sigma(x) J_{-\sigma}(x)\right),$$

$$G_{21} = -\,G_{12}\,, \qquad G_{31} = +\,G_{13}, \quad G_{32} = -\,G_{23}. \tag{65}$$

The elements Q_{ab}, and then the matrix elements M_{ij}, are given in terms of these coefficients in equation (63). The variable σ being positive, it is useful to eliminate the Bessel functions of negative indices for other Bessel functions with positive indices. This is possible since the Bessel function of the first kind and negative index $J_{-\sigma}(x)$ can be expressed in terms of Bessel functions of the first and second kind with positive indices, $J_\sigma(x)$ and $N_\sigma(x)$ by the left identity in equation (66) below (Abramowitz & Stegun 1964). When derivatives are involved, the second relation in equation (66), that gives the Wronskian of the functions of the first and second kind (Abramowitz & Stegun 1964), may be used to eliminate N'_σ if needed. We then base the transformation to positive σ values on the relations:

$$J_{-\sigma}(x) = \cos\sigma\pi\, J_\sigma(x) - \sin\sigma\pi N_\sigma(x), \qquad J_\sigma(x) N'_\sigma(x) - J'_\sigma(x) N_\sigma(x) = \frac{2}{\pi x}. \tag{66}$$

Using equation (66), the elements Q_{ab} in equation (63) can all be expressed in terms of $J_\sigma(x)$, $N_\sigma(x)$ and their derivatives with respect to x. Some components of these expressions turn out to be regular at integer values of σ, while some other keep a singular denominator $\sin\sigma\pi$ which generates expressions that must, again, be understood in the sense of distributions. The matrix elements M_{ij} in equations (61) and (62) can then be explicitly written as

$$
\begin{aligned}
M_{XX} &= (+\mathrm{i}) \lim_{N\to\infty}\left(1-\mathrm{e}^{2\mathrm{i}\pi N\sigma}\right) \quad \frac{v_\perp}{|\,\Omega_*|}\left(\omega\frac{\partial f_0}{\partial p_\perp}+k_\parallel D(f_0)\right) \qquad \pi\frac{\sigma^2}{x^2}\left(\frac{\cos\sigma\pi}{\sin\sigma\pi}J_\sigma^2(x)-J_\sigma(x)N_\sigma(x)-\frac{1}{\sigma\pi}\right),\\
M_{XY} &= (-s_q) \lim_{N\to\infty}\left(1-\mathrm{e}^{2\mathrm{i}\pi N\sigma}\right) \quad \frac{v_\perp}{|\,\Omega_*|}\left(\omega\frac{\partial f_0}{\partial p_\perp}+k_\parallel D(f_0)\right) \qquad \pi\frac{\sigma}{x}\left(\frac{\cos\sigma\pi}{\sin\sigma\pi}J_\sigma(x)J'_\sigma(x)-J'_\sigma(x)N_\sigma(x)-\frac{1}{\pi x}\right),\\
M_{XZ} &= (+\mathrm{i}) \lim_{N\to\infty}\left(1-\mathrm{e}^{2\mathrm{i}\pi N\sigma}\right) \quad \frac{v_\perp}{|\,\Omega_*|}\left(\omega\frac{\partial f_0}{\partial p_\parallel}-k_\perp D(f_0)\frac{\sigma}{x}\right) \qquad \pi\frac{\sigma}{x}\left(\frac{\cos\sigma\pi}{\sin\sigma\pi}J_\sigma^2(x)-J_\sigma(x)N_\sigma(x)-\frac{1}{\sigma\pi}\right),\\
M_{YX} &= (+s_q) \lim_{N\to\infty}\left(1-\mathrm{e}^{2\mathrm{i}\pi N\sigma}\right) \quad \frac{v_\perp}{|\,\Omega_*|}\left(\omega\frac{\partial f_0}{\partial p_\perp}+k_\parallel D(f_0)\right) \qquad \pi\frac{\sigma}{x}\left(\frac{\cos\sigma\pi}{\sin\sigma\pi}J_\sigma(x)J'_\sigma(x)-J'_\sigma(x)N_\sigma(x)-\frac{1}{\pi x}\right) \qquad (67)\\
M_{YY} &= (+\mathrm{i}) \lim_{N\to\infty}\left(1-\mathrm{e}^{2\mathrm{i}\pi N\sigma}\right) \quad \frac{v_\perp}{|\,\Omega_*|}\left(\omega\frac{\partial f_0}{\partial p_\perp}+k_\parallel D(f_0)\right) \qquad \pi\left(\frac{\cos\sigma\pi}{\sin\sigma\pi}J'^2_\sigma(x)-J'_\sigma(x)N'_\sigma(x)+\frac{\sigma}{\pi x^2}\right),\\
M_{YZ} &= (+s_q) \lim_{N\to\infty}\left(1-\mathrm{e}^{2\mathrm{i}\pi N\sigma}\right) \quad \frac{v_\perp}{|\,\Omega_*|}\left(\omega\frac{\partial f_0}{\partial p_\parallel}-k_\perp D(f_0)\frac{\sigma}{x}\right) \qquad \pi\left(\frac{\cos\sigma\pi}{\sin\sigma\pi}J_\sigma(x)J'_\sigma(x)-J'_\sigma(x)N_\sigma(x)-\frac{1}{\pi x}\right),\\
M_{ZX} &= (+\mathrm{i}) \lim_{N\to\infty}\left(1-\mathrm{e}^{2\mathrm{i}\pi N\sigma}\right) \quad \frac{v_\parallel}{|\,\Omega_*|}\left(\omega\frac{\partial f_0}{\partial p_\perp}+k_\parallel D(f_0)\right) \qquad \pi\frac{\sigma}{x}\left(\frac{\cos\sigma\pi}{\sin\sigma\pi}J_\sigma^2(x)-J_\sigma(x)N_\sigma(x)-\frac{1}{\pi\sigma}\right),\\
M_{ZY} &= (-s_q) \lim_{N\to\infty}\left(1-\mathrm{e}^{2\mathrm{i}\pi N\sigma}\right) \quad \frac{v_\parallel}{|\,\Omega_*|}\left(\omega\frac{\partial f_0}{\partial p_\perp}+k_\parallel D(f_0)\right) \qquad \pi\left(\frac{\cos\sigma\pi}{\sin\sigma\pi}J_\sigma(x)J'_\sigma(x)-J'_\sigma(x)N_\sigma(x)-\frac{1}{\pi x}\right),\\
M_{ZZ} &= (+\mathrm{i}) \lim_{N\to\infty}\left(1-\mathrm{e}^{2\mathrm{i}\pi N\sigma}\right) \quad \frac{v_\parallel}{|\,\Omega_*|}\left(\left(\omega\frac{\partial f_0}{\partial p_\parallel}-k_\perp D(f_0)\frac{\sigma}{x}\right)\pi\left(\frac{\cos\sigma\pi}{\sin\sigma\pi}J_\sigma^2(x)-J_\sigma(x)N_\sigma(x)\right)+\frac{1}{x}k_\perp D(f_0)\right). \qquad (68)
\end{aligned}
$$

Let us now specify the meaning of $\lim\left(1-\mathrm{e}^{2\mathrm{i}\pi N\sigma}\right)$, which enters with other factors in integrals over σ implied by the integration over momenta in equation (61). When this factor multiplies a regular function of σ, its limit is unity since, when N diverges, $\exp(2\mathrm{i}\pi N\sigma)$ oscillates infinitely rapidly leaving in the limit a vanishing integral when multiplied by any regular function. The case when a factor $(\cos\sigma/\sin\sigma\pi)$ multiplies $(1-\exp(2\mathrm{i}\pi N\sigma))$ deserves closer scrutiny, since both $\sin\sigma\pi$ and $(1-\exp(2\mathrm{i}\pi N\sigma))$ vanish at integer values. It is shown in Appendix C that the limit of their product is the distribution

$$
\lim_{N\to\infty}\left(1-\mathrm{e}^{2\mathrm{i}\pi N\sigma}\right)\frac{\cos\sigma\pi}{\sin\sigma\pi} \;\equiv\; \mathcal{D}\Big(\frac{\cos\sigma\pi}{\sin\sigma\pi}\Big) \;=\; \left(\mathcal{P}\Big(\frac{\cos\sigma\pi}{\sin\sigma\pi}\Big)-\mathrm{i}\sum_{n\in\mathbb{N}}\delta_{\mathrm{D}}(\sigma-n)\right), \qquad (69)
$$

where $\mathbb{N}$ is the set of positive integers, δ_{D} a Dirac distribution and the notation $\mathcal{P}$ means that the function which follows in the parentheses should be taken as a Cauchy principal value near each of its singularities, which in this case are the integer values of σ. The effect of the multiple resonances at all integer values of σ that are involved in the matrix elements of the conductivity is concentrated on those terms in equation (68) in which factors $(\cos\sigma\pi/\sin\sigma\pi)$ subsist, although it could have been expected that resonances should be present in all terms since equation (64) exhibits such a singular factor. In changing according to equation (66) for Bessel functions with positive indices only, some of these singular factors have been disposed of, having been regularized owing to the favourably phased term proportional to $\sin\sigma\pi\, N_\sigma(x)$ in equation (66). This means that the transformation to Bessel functions with only positive indices has allowed to carry out the summation over resonances for these favourably phased terms. Resonances only remain explicitly present in the unfavourably phased ones, that originate in the term $\cos\sigma\pi\, J_\sigma(x)$ in equation (66). It is shown in Section 4.4 that these residual resonant terms eventually turn out to be negligible when $\omega/|\Omega|\gg 1$.

4.2 Polarization transfer coefficients from the conductivity

The elements of the transfer matrix are given in equation (12) in terms of the components of the conductivity tensor in the plane perpendicular to the direction of propagation of the radiation. Since the components of this tensor are known in a frame in which the static magnetic field is along the Z-axis, the components in equation (68) must be transformed to the new reference frame x', y', z' represented in Fig. 5 in which the wave vector $\boldsymbol{k}$ is along the z'-axis. For our purpose, it suffices to calculate the transverse components $x'x'$, $x'y'$, $y'x'$, $y'y'$ which are given by Thiébaut (2010)

$$
M_{x'x'}=M_{YY}\,, \qquad M_{x'y'}=\sin\alpha\, M_{YZ}-\cos\alpha\, M_{YX}\,, \qquad M_{y'x'}=\sin\alpha\, M_{ZY}-\cos\alpha\, M_{XY}, \qquad (70)
$$

$$
M_{y'y'}=\cos^2\alpha\, M_{XX}+\sin^2\alpha\, M_{ZZ}-\sin\alpha\cos\alpha\,(M_{ZX}+M_{XZ}). \qquad (71)
$$

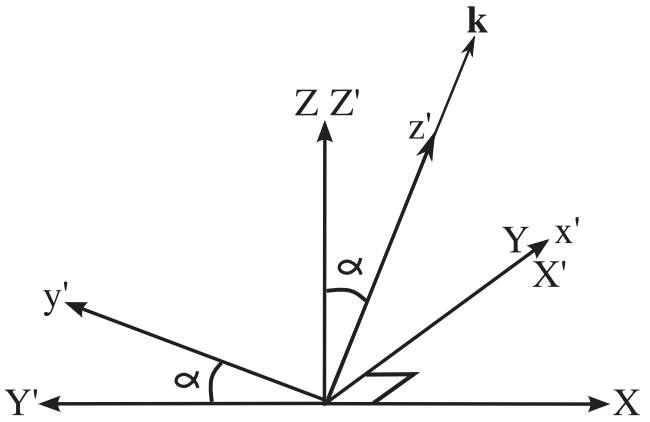

Figure 5. The Z-axis is along the unperturbed magnetic field. The z'-axis is along the wave vector $\boldsymbol{k} = k\cos\alpha\,\boldsymbol{e}_Z + k\sin\alpha\,\boldsymbol{e}_X$, where $0 \le \alpha \le \pi$. The axes Y and x' are identical.

These calculations are straightforward, but it nevertheless takes some algebra to reduce them to the simple form in equations (72)–(74). Some details are given in Appendix D. The transverse components of the **M** matrix can eventually be written as

$$M_{x'x'} = \frac{\mathrm{i}\pi}{\gamma m}\, x^2\, \frac{\partial f_0}{\partial \sigma}\left(\mathcal{D}\left(\frac{\cos\sigma\pi}{\sin\sigma\pi}\right) J'^2_\sigma(x) - J'_\sigma(x) N'_\sigma(x) + \frac{\sigma}{\pi x^2}\right). \tag{72}$$

$$M_{x'y'} = -\frac{s_q \pi}{\gamma m}\,\varpi\, x\, \frac{\partial f_0}{\partial \sigma}\left(\mathcal{D}\left(\frac{\cos\sigma\pi}{\sin\sigma\pi}\right) J_\sigma(x) J'_\sigma(x) - J'_\sigma(x) N_\sigma(x) - \frac{1}{\pi x}\right), \qquad M_{y'x'} = -M_{x'y'}. \tag{73}$$

$$M_{y'y'} = \frac{\mathrm{i}\pi}{\gamma m}\,\varpi^2\, \frac{\partial f_0}{\partial \sigma}\left(\mathcal{D}\left(\frac{\cos\sigma\pi}{\sin\sigma\pi}\right) J^2_\sigma(x) - J_\sigma(x) N_\sigma(x)\right) - \frac{\mathrm{i}}{\gamma m}\left((\sigma\cos\alpha - \varpi)\, \frac{\partial f_0}{\partial \varpi} + \varpi\,\cos\alpha\, \frac{\partial f_0}{\partial \sigma}\right). \tag{74}$$

From equations (72)–(74), we may calculate the corresponding components of the conductivity. The density n of the particles is factored out of the distribution function by writing it as $f_0 = nF_0$, defining a reduced distribution function normalized to unity and a plasma frequency ω_{pr} for the relativistic species of particles considered:

$$f_0 = n\,F_0\,, \qquad \int_0^\infty 2\pi p_\perp \mathrm{d}p_\perp \int_{-\infty}^{+\infty} \mathrm{d}p_\parallel F_0 = 1\,, \qquad \omega_{\mathrm{pr}}^2 = \frac{nq^2}{\varepsilon_0 m}. \tag{75}$$

The components of the anti-Hermitian and Hermitian parts of the conductivity can then be written as

$$\frac{\sigma^A_{x'x'}}{\varepsilon_0} = -2\pi^2 \mathrm{i}\frac{\omega_{\mathrm{pr}}^2\Omega^2}{\omega^3} \iint \frac{m^3c^3}{\sin^2\alpha}\,\mathrm{d}\varpi\,\mathrm{d}\sigma\; x^2 \frac{\partial F_0}{\partial \sigma}\left(\mathcal{P}\left(\frac{\cos\sigma\pi}{\sin\sigma\pi}\right) J'^2_\sigma(x) - J'_\sigma(x) N'_\sigma(x) + \frac{\sigma}{\pi x^2}\right), \tag{76}$$

$$\frac{\sigma^A_{x'y'}}{\varepsilon_0} = +2\pi^2 s_q \frac{\omega_{\mathrm{pr}}^2\Omega^2}{\omega^3} \iint \frac{m^3c^3}{\sin^2\alpha}\,\mathrm{d}\varpi\,\mathrm{d}\sigma\;\varpi x \frac{\partial F_0}{\partial \sigma}\left(\mathcal{P}\left(\frac{\cos\sigma\pi}{\sin\sigma\pi}\right) J_\sigma(x) J'_\sigma(x) - J'_\sigma(x) N_\sigma(x) - \frac{1}{\pi x}\right), \qquad \sigma^A_{y'x'} = -\sigma^A_{x'y'}, \tag{77}$$

$$\frac{\sigma^A_{y'y'}}{\varepsilon_0} = -2\pi^2 \mathrm{i}\frac{\omega_{\mathrm{pr}}^2\Omega^2}{\omega^3} \iint \frac{m^3c^3}{\sin^2\alpha}\,\mathrm{d}\varpi\,\mathrm{d}\sigma\left[\varpi^2 \frac{\partial F_0}{\partial \sigma}\left(\mathcal{P}\left(\frac{\cos\sigma\pi}{\sin\sigma\pi}\right) J^2_\sigma(x) - J_\sigma N_\sigma(x)\right) - \frac{1}{\pi}\left((\sigma\cos\alpha - \varpi)\frac{\partial F_0}{\partial \varpi} + \varpi\cos\alpha \frac{\partial F_0}{\partial \sigma}\right)\right], \tag{78}$$

$$\frac{\sigma^H_{x'x'}}{\varepsilon_0} = -2\pi^2 \frac{\omega_{\mathrm{pr}}^2\Omega^2}{\omega^3} \sum_{n\in\mathbb{N}} \iint \frac{m^3c^3}{\sin^2\alpha}\,\mathrm{d}\varpi\,\mathrm{d}\sigma\; x^2 \frac{\partial F_0}{\partial \sigma} J'^2_\sigma(x)\,\delta_{\mathrm{D}}(\sigma - n), \tag{79}$$

$$\frac{\sigma^H_{x'y'}}{\varepsilon_0} = -2\pi^2 \mathrm{i} s_q \frac{\omega_{\mathrm{pr}}^2\Omega^2}{\omega^3} \sum_{n\in\mathbb{N}} \iint \frac{m^3c^3}{\sin^2\alpha}\,\mathrm{d}\varpi\,\mathrm{d}\sigma\;\varpi x \frac{\partial F_0}{\partial \sigma} J_\sigma(x) J'_\sigma(x)\,\delta_{\mathrm{D}}(\sigma - n)\,, \qquad \sigma^H_{y'x'} = -\sigma^H_{x'y'}, \tag{80}$$

$$\frac{\sigma^H_{y'y'}}{\varepsilon_0} = -2\pi^2 \frac{\omega_{\mathrm{pr}}^2\Omega^2}{\omega^3} \sum_{n\in\mathbb{N}} \iint \frac{m^3c^3}{\sin^2\alpha}\,\mathrm{d}\varpi\,\mathrm{d}\sigma\;\varpi^2 \frac{\partial F_0}{\partial \sigma} J^2_\sigma(x)\,\delta_{\mathrm{D}}(\sigma - n). \tag{81}$$

The elements of the transfer matrix in equation (1) can be found from these results by using equation (12). Our choice of reference axes in the plane perpendicular to $\boldsymbol{k}$ results in the vanishing of the coefficients K_{QV} and K_{IU}, since $\sigma^A_{x'y'}$ is real and $\sigma^H_{x'y'}$ is imaginary. In equation (78) the integration over ϖ and σ of the terms $\cos\alpha(\sigma\,\partial_\varpi F_0 + \varpi\,\partial_\sigma F_0)$ can be reduced to an integral on the boundary of the physical domain which vanishes.

4.3 Formal expression of the polarization transfer coefficients

The components of the Hermitian part of the conductivity in equations (79)–(81) are associated with dissipative radiative effects. Equation (12) relates them to the absorption coefficients per unit time which appear in equation (1). The transfer coefficients per unit length in a medium of negligible dispersion are obtained from them by dividing by the velocity of light. The discrete sum over the large positive integers n in equations (79)–(81) can be approximated by an integral, so that

$$\frac{K_{II}}{c} = -\pi^2 \frac{\omega_{\rm pr}^2 \Omega^2}{c\omega^3} \iint \frac{m^3 c^3}{\sin^2\alpha}\, {\rm d}\varpi\, {\rm d}\sigma\, \frac{\partial F_0}{\partial \sigma} \left[x^2 J_\sigma'^2(x) + \varpi^2 J_\sigma^2(x)\right], \tag{82}$$

$$\frac{K_{IQ}}{c} = -\pi^2 \frac{\omega_{\rm pr}^2 \Omega^2}{c\omega^3} \iint \frac{m^3 c^3}{\sin^2\alpha}\, {\rm d}\varpi\, {\rm d}\sigma\, \frac{\partial F_0}{\partial \sigma} \left[x^2 J_\sigma'^2(x) - \varpi^2 J_\sigma^2(x)\right], \tag{83}$$

$$\frac{K_{IV}}{c} = -2\pi^2 s_q \frac{\omega_{\rm pr}^2 \Omega^2}{c\omega^3} \iint \frac{m^3 c^3}{\sin^2\alpha}\, {\rm d}\varpi\, {\rm d}\sigma\, \frac{\partial F_0}{\partial \sigma}\, \varpi x J_\sigma(x) J_\sigma'(x). \tag{84}$$

We return to the dissipative coefficients in Section 5.2. There are two non-dissipative coefficients, which in a stationary medium are usually defined per unit length. Assuming again no dispersion, they are $f = K_{QU}/c$ and $h = K_{UV}/c$. When acting alone on radiation propagating in the direction of the unit vector $\boldsymbol{n}$, they cause the Stokes parameters Q, U, V to vary according to

$$\boldsymbol{n}\cdot\nabla \begin{pmatrix} I \\ Q \\ U \\ V \end{pmatrix} = - \begin{pmatrix} 0 & 0 & 0 & 0 \\ 0 & 0 & f & 0 \\ 0 & -f & 0 & h \\ 0 & 0 & -h & 0 \end{pmatrix} \begin{pmatrix} I \\ Q \\ U \\ V \end{pmatrix}. \tag{85}$$

This simplified transfer equation leaves the intensity I invariant as well as the degree of polarization $\sqrt{Q^2+U^2+V^2}/I$. The argument of all Bessel functions implicitly being x, the coefficients f and h can be written as

$$f = 2\pi^2 s_q \frac{\omega_{\rm pr}^2 \Omega^2}{c\,\omega^3} \iint \frac{m^3 c^3}{\sin^2\alpha}\, {\rm d}\varpi\, {\rm d}\sigma\ \ \varpi\, x\, \frac{\partial F_0}{\partial \sigma} \left[\mathcal{P}\left(\frac{\cos\sigma\pi}{\sin\sigma\pi}\right) J_\sigma J_\sigma' - J_\sigma' N_\sigma - \frac{1}{\pi x}\right], \tag{86}$$

$$h = \pi^2 \frac{\omega_{\rm pr}^2 \Omega^2}{c\,\omega^3} \iint \frac{m^3 c^3}{\sin^2\alpha}\, {\rm d}\varpi\, {\rm d}\sigma \left[\frac{\partial F_0}{\partial \sigma}\left(\mathcal{P}\left(\frac{\cos\sigma\pi}{\sin\sigma\pi}\right)\left(\varpi^2 J_\sigma^2 - x^2 J_\sigma'^2\right) + \left(x^2 J_\sigma' N_\sigma' - \varpi^2 J_\sigma N_\sigma\right)\right) + \frac{1}{\pi}\left(\varpi \frac{\partial F_0}{\partial \varpi} - \sigma \frac{\partial F_0}{\partial \sigma}\right)\right]. \tag{87}$$

4.4 The residual contribution of resonances to non-dissipative coefficients is negligible

The principal value terms in equations (86) and (87) are negligible in the limit $\omega \gg |\Omega|$ in which σ and x are large. To prove this, we use the fact that the interval between successive zeros of $\sin\sigma\pi$ is unity, whereas the Bessel functions vary on a much longer scale because both their index and argument are large, the argument remaining smaller than their index, though. This can be seen from the definition of σ and x in equation (23). The contribution to the integral over σ of each unit interval $[n-\frac{1}{2}, n+\frac{1}{2}]$ can then be calculated at any accuracy by Taylor-expanding about n the function which factors $\cot\sigma\pi$ in equations (86) and (87). This provides the result of the integration on $[n-\frac{1}{2}, n+\frac{1}{2}]$ in the form of a series. The summation of these functions of n over all unit intervals centred on integer values can then be approximately replaced, provided σ is large, by an integral over σ since they slowly vary with n. This integral turns out to be extremely small, owing to particular properties of the functions $J_\sigma(x)$ and $J_\sigma'(x)$ for large σ and small x. Details are to be found in Appendix E. With this further simplification, the polarization transfer coefficients in equations (86) and (87) lose their principal value terms. Terms in which no Bessel functions are involved can be reduced to a line integral on the boundary $\mathcal{B}$ of the physical domain in the ϖ–σ plane (Appendix A), which is particularly useful to transform equation (87) in which the term devoid of Bessel functions is the divergence of the vector with components $v_\varpi = \varpi F_0$ and $v_\sigma = -\sigma F_0$. All calculations done, we get

$$f = -\frac{2\pi^2 s_q}{c} \frac{\omega_{\rm pr}^2 \Omega^2}{\omega^3} \iint \frac{m^3 c^3}{\sin^2\alpha}\, {\rm d}\varpi\, {\rm d}\sigma\ \ \varpi\, x\ \left(J_\sigma'(x) N_\sigma(x) + \frac{1}{\pi x}\right) \frac{\partial F_0}{\partial \sigma}, \tag{88}$$

$$h = \frac{\pi^2 \omega_{\rm pr}^2 \Omega^2}{c\,\omega^3} \iint \frac{m^3 c^3}{\sin^2\alpha}\, {\rm d}\varpi\, {\rm d}\sigma \left(x^2 J_\sigma'(x) N_\sigma'(x) - \varpi^2 J_\sigma(x) N_\sigma(x)\right) \frac{\partial F_0}{\partial \sigma} + \frac{\pi \omega_{\rm pr}^2 \Omega^2}{c\,\omega^3} \int_{-\infty}^{+\infty} \frac{m^3 c^3}{\sin^2\alpha}\, {\rm d}\varpi\ \ \frac{2\varpi^2 + \sigma_0^2}{\sqrt{\varpi^2 + \sigma_0^2}} F_0(\varpi, \sigma_b(\varpi)). \tag{89}$$

The notation $\sigma_b(\varpi) = \sqrt{\sigma_0^2 + \varpi^2}$ denotes the value of σ at a point of abscissa ϖ on the boundary $\mathcal{B}$ of the physical domain in the ϖ–σ plane. It will soon be shown that, when expanding the Bessel functions in $|\Omega|/\omega$, the non-Bessel terms in equations (88) and (89) almost exactly cancel the zeroth-order terms of the development. Equations (88) and (89) are applicable to any distribution function. The integrals over σ and/or ϖ extend to the full range of physically relevant values and no other approximation has been made than neglecting the series of

residual principal value terms, which is well justified. Equations (88) and (89) are then close to being exact. They however feature complicated kernels, which makes it desirable to find simpler and suitable approximations to them.

5 NR AND QR PARTS OF THE TRANSFER COEFFICIENTS

5.1 QR contribution to transfer coefficients from Nicholson's approximation

The phase integrals in equation (22) involve the integration of trigonometric functions which may vary more or less rapidly with the delay time τ, depending on the values of the particle's parameters and the gyration angle ϕ. Let us denote by ϑ the pitch angle of a particle, that is, the angle of the particle's velocity with the magnetic field. According to equation (22), the characteristic variation frequency of the phase most often is of the order of ω. When however the modulus of the particle's velocity is close to the speed of light, the characteristic frequency of phase variations may occasionally be much less, when the angle between the particle's velocity and the wave vector becomes small enough. For example, equation (22) indicates that this frequency would be of the order of $|\Omega|$ or less when

$$\omega - k_\parallel v_\parallel - k_\perp v_\perp \cos\phi \ \le |\,\Omega\,|\,, \qquad \text{that is} \qquad \left(1-\frac{v}{c}\right)+\frac{v}{c}\,(1-\cos(\vartheta-\alpha))+\frac{v}{c}\sin\alpha\sin\vartheta\,(1-\cos\phi) \ \le \ \frac{|\,\Omega\,|}{ck}. \tag{90}$$

Since $u = ck/|\Omega|$ is very large, this requires that each term on the left of the second inequality in equation (90) be less than the term on the right, i.e. that

$$|\alpha-\vartheta| \le \left(\frac{|\Omega|}{\omega}\right)^{1/2}, \qquad |\phi| \le \left(\frac{|\Omega|}{\omega}\right)^{1/2}, \qquad (1/\gamma) \ \le \ \left(\frac{|\Omega|}{\omega}\right)^{1/2}. \tag{91}$$

For quasi-resonance, the third inequality in equation (91) requires that ω should be less than $\gamma^2|\Omega|$ which is of the order of the characteristic frequency of the synchrotron emission spectrum by a particle of Lorentz factor γ (equation 101). The other inequalities in equation (91) require that the angle between the wave vector and the particle's velocity be, for a frequency at the peak of synchrotron emission, less than $1/\gamma$. These inequalities are only satisfied by a restricted class of particles, which we refer to as QR particles. For QR particles, the characteristic frequency of the variations of the phase [the integrand in equation (22)] is, during a small fraction of the synchrotron gyration period, much less than ω and, because of this slow variation with τ, the phase integral is exceptionally large.

This induced some authors (Sazonov 1969b; Heyvaerts 1970; Melrose 1997c,d) to consider that QR particles entirely determine the non-dissipative transfer coefficients, just as they determine the dissipative ones and the emission coefficients (Westfold 1959). This shows up when phase integrals are evaluated by the method of the (quasi-) stationary phase, resulting in the presence in the results of Airy-type functions. The dominance of the contribution of QR particles to non-dissipative transfer coefficients is however not granted. The functions which determine the dissipative coefficients in equations (79)–(81) happen to be vanishingly small for NR particles, but those determining the non-dissipative ones have a much wider support and are associated with a large number of NR particles. At this point, we do not know whether the QR contribution to the non-dissipative coefficients is negligible compared to the NR one, or comparable to it. This will be discussed in Section 5.4.

The first inequality in equation (90), which defines QR particles, can be written for $\phi = 0$ in terms of the variables σ and x in equation (23) as $(\sigma - x) < \gamma$. The pitch angle ϑ of the particle and the propagation angle α of the wave being almost equal at quasi-resonance, $\sigma \approx \gamma u \sin^2\alpha$. Considering the general case when α is not very small, this yields $\sigma \sim \gamma u$, a very large value. Imposing the condition $(\sigma - x) < \gamma$ to a wave with frequency in the peak of the synchrotron emission, such that $\omega \sim \gamma^2|\Omega|$, we get $\sigma \approx \gamma^3$, which then implies that for quasi-resonance

$$\frac{\sigma - x}{\sigma} < \frac{1}{\sigma^{2/3}}. \tag{92}$$

Thus, for QR particles, σ and x are very close to each other, x being however slightly smaller, since, from equation (23), $(\sigma - x)$ must be positive. The inequality in equation (92) places the argument x in the intermediate region where the so-called Nicholson's approximation to Bessel functions of large index and argument is appropriate (Watson 1922, chapter 8; Olver 1952). Nicholson's approximation to $J_\sigma(x)$ is well known but the corresponding approximation to $N_\sigma(x)$ is not. Its derivation is outlined in Appendix F. The functions J_σ, N_σ and their derivatives may be represented in this range by modified Bessel functions of the second kind $K_\nu(g)$, with index $\nu = 1/3$ or $2/3$, and by a similar combination $L_\nu(g)$ of modified Bessel functions of the first kind, $I_{\pm\nu}(g)$. K_ν and L_ν are defined by

$$K_\nu(g) = \frac{\pi}{2}\,\frac{I_{-\nu}(g) - I_\nu(g)}{\sin\nu\pi}\,, \qquad L_\nu(g) = \frac{\pi}{2}\,\frac{I_{-\nu}(g) + I_\nu(g)}{\sin\nu\pi}. \tag{93}$$

The definition of the functions K_ν is standard (Abramowitz & Stegun 1964) and applies to integer values of the index in a limit sense. Our definition of the functions L_ν in equation (93) does not make sense for integer ν. However, we only deal here with indices $\nu = 1/3$ or $2/3$. The argument g on which these functions depend is

$$g = \frac{2^{3/2}}{3}\,\frac{(\sigma - x)^{3/2}}{x^{1/2}}. \tag{94}$$

From equation (92), it can be seen that the variable g is $\mathcal{O}(1)$ or smaller wherever Nicholson's approximation applies. The latter yields the following approximate representations:

$$J_\sigma(x) \approx \frac{1}{\pi}\sqrt{\frac{2}{3}}\sqrt{\frac{\sigma-x}{x}}\,K_{\frac{1}{3}}(g)\,, \qquad N_\sigma(x) \approx -\frac{\sqrt{2}}{\pi}\sqrt{\frac{\sigma-x}{x}}\,L_{\frac{1}{3}}(g), \tag{95}$$

$$J'_\sigma(x) \approx \frac{2}{\pi\sqrt{3}}\left(\frac{\sigma-x}{x}\right)K_{\frac{2}{3}}(g)\,, \qquad N'_\sigma(x) \approx \frac{2}{\pi}\left(\frac{\sigma-x}{x}\right)L_{\frac{2}{3}}(g). \tag{96}$$

The QR contributions to the Faraday coefficients f and h are obtained by substituting equations (95) and (96) into equations (88) and (89), the domain of integration in the ϖ–σ plane then being restricted to the QR one. This domain is characterized by the inequality in equation (92), or equivalently, since at quasi-resonance x and σ are nearly equal, by the requirement that the variable g in equation (94) be less than or equal to unity. From equations (94) and (A2), the condition that $g = 1$ translates into

$$\varpi^2 + \sigma_0^2 = 3^{2/3}\sigma^{4/3}. \tag{97}$$

The variable g can then be less than unity only when σ exceeds a threshold $\sigma_{\rm QR}$ and the Lorentz factor exceeds a related one, $\gamma_{\rm QR}$, such that the line $\gamma = \gamma_{\rm QR}$ in Fig. 6 be tangent to the boundary $\mathcal{B}_{\rm QR}$. The Lorentz factor $\gamma_{\rm QR}$ is of the order of the γ variable associated with $\sigma_{\rm QR}$ and $\varpi = 0$. To sum up,

$$\sigma_{\rm QR} = \frac{\sigma_0^{3/2}}{\sqrt{3}}\,, \qquad \gamma_{\rm QR} \approx \sqrt{\frac{u}{3\sin\alpha}}. \tag{98}$$

Thus, a particle can only quasi-resonantly interact with the radiation when σ exceeds $\sigma_{\rm QR}$. Since σ_0 defined in equation (23) is usually large, $\sigma_{\rm QR} \gg \sigma_0$. The characteristic frequency $\omega_c(\gamma, \alpha)$ of synchrotron emission by particles of Lorentz factor $\gamma_{\rm QR}$, defined in equation (101), is almost ω. Fig. 6 represents the QR domain in the ϖ–σ plane. When $u = \omega/|\Omega|$ becomes very large, $\sigma_{\rm QR}$ diverges as $u^{3/2}$ while the σ value corresponding to a given Lorentz factor γ diverges as u. This means that at high enough frequency there will be a negligible number of particles in quasi-resonance and the transfer coefficients will then be essentially given by the NR contribution. When on the contrary $\sigma > \sigma_{\rm QR}$ for relevant values of γ, the QR region partly contributes to f and h. These contributions are

$$f_{\rm QR} = 2s_q\,\frac{\omega_{\rm pr}^2\Omega^2}{c\,\omega^3}\iint_{\rm QR}\frac{m^3c^3}{\sin^2\alpha}\,{\rm d}\varpi\,{\rm d}\sigma\;\varpi\,x\left(\frac{2\sqrt{2}}{\sqrt{3}}\left(\frac{\sigma-x}{x}\right)^{\frac{3}{2}}K_{\frac{2}{3}}(g)L_{\frac{1}{3}}(g) - \frac{\pi}{x}\right)\frac{\partial F_0}{\partial\sigma}, \tag{99}$$

$$h_{\rm QR} = \frac{\omega_{\rm pr}^2\Omega^2}{c\,\omega^3}\iint_{\rm QR}\frac{m^3c^3}{\sin^2\alpha}\,{\rm d}\varpi\,{\rm d}\sigma\left(\frac{4x^2}{\sqrt{3}}\left(\frac{\sigma-x}{x}\right)^2K_{\frac{2}{3}}(g)L_{\frac{2}{3}}(g) + \frac{2\varpi^2}{\sqrt{3}}\left(\frac{\sigma-x}{x}\right)K_{\frac{1}{3}}(g)L_{\frac{1}{3}}(g)\right)\frac{\partial F_0}{\partial\sigma}, \tag{100}$$

where the subscript QR indicates that the integration should be carried over the QR domain only.

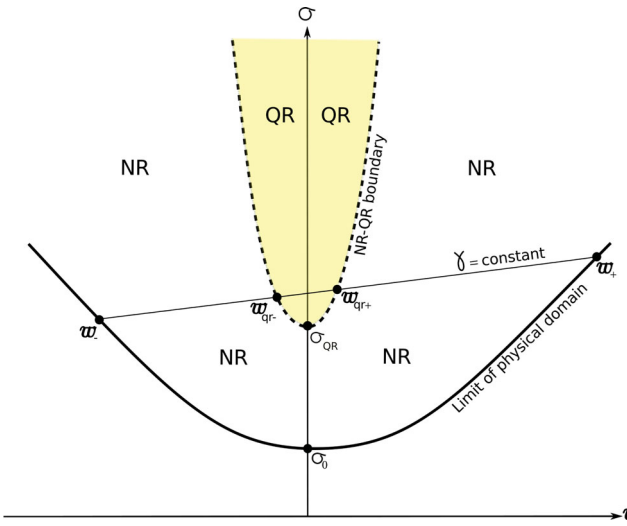

Figure 6. The physical domain of the ϖ–σ plane is above the hyperbolic line $\mathcal{B}$, of equation $\sigma^2 = \varpi^2 + \sigma_0^2$. The smallest possible value of σ is $\sigma_0 = \omega\sin\alpha/|\Omega|$. The QR domain is the yellow shaded area defined by $g \leq 1$ (equation 94). It is bounded by the dashed line $\mathcal{B}_{\rm QR}$, represented by equation (97). The smallest value $\sigma_{\rm QR}$ of σ on $\mathcal{B}_{\rm QR}$, denoted by $\sigma_{\rm QR}$ in the figure, is given by equation (97) for $\varpi = 0$. The oblique line is the locus of a constant value of the Lorentz factor γ. It intersects $\mathcal{B}$ at $\varpi = \varpi_-(\gamma)$ and $\varpi_+(\gamma)$ and $\mathcal{B}_{\rm QR}$ at $\varpi = \varpi_{\rm QR-}(\gamma)$ and $\varpi_{\rm QR+}(\gamma)$.

5.2 Polarization-dependent absorption coefficients

The dissipative coefficients per unit length are given by equations (82)–(84). Since the product of Bessel functions declines exponentially out of the QR domain, it is appropriate to use Nicholson's approximation to represent them (equations 94–96). Equations (82)–(84) are then expressed in terms of the Lorentz factor γ and the pitch angle ϑ of the particles, or the difference ψ of the latter and the propagation angle α, which remains small in the QR domain. This results in $\partial_\sigma F_0 \approx (\partial_\gamma F_0 - \psi\, \partial_\vartheta F_0/\gamma)/u \sin^2\alpha$. Owing to the smallness of ψ, the angular derivative term may sometimes be neglected. Similarly, the argument g of the K Bessel functions in equations (95) and (96) may sometimes be approximated by $g_0 \approx (\omega/3\gamma^2\Omega\sin\alpha)\,(1+\gamma^2\psi^2)^{3/2}$. The critical frequency ω_c of synchrotron emission by a particle of Lorentz factor γ in the direction α is defined by (Westfold 1959)

$$\omega_c = \frac{3}{2}\,\gamma^2\,|\,\Omega\,|\,\sin\alpha. \tag{101}$$

The integration over the particles' directions on the right-hand sides of equations (82)–(84) can be performed as in Westfold (1959), which gives for the total and linear polarization absorption coefficients:

$$\frac{K_{II}}{c} = -\frac{\omega_{\rm pr}^2\,|\,\Omega\,|}{c\,\omega^2}\frac{\sqrt{3}\,\pi}{2}\,\sin\alpha\int m^3c^3\,\gamma^2\,{\rm d}\gamma\,\frac{\partial F_0}{\partial\gamma}\;\frac{\omega}{\omega_c}\int_{\frac{\omega}{\omega_c}}^{\infty}K_{5/3}(u)\,{\rm d}u, \tag{102}$$

$$\frac{K_{IQ}}{c} = -\frac{\omega_{\rm pr}^2\,|\,\Omega\,|}{c\,\omega^2}\frac{\sqrt{3}\,\pi}{2}\,\sin\alpha\int m^3c^3\,\gamma^2\,{\rm d}\gamma\;\frac{\partial F_0}{\partial\gamma}\;\frac{\omega}{\omega_c}K_{2/3}\left(\frac{\omega}{\omega_c}\right). \tag{103}$$

Here, $\partial_\gamma F_0$ is meant to be taken at $\vartheta=\alpha$, the propagation angle. The results (102) and (103) coincide with those of Sazonov (1969a), considering his use of the CGS system of units, the definition of his distribution function, and the presence of an unfortunate typo in the first part of his equation 2.2, where $\int_{\nu/\nu_c}^{\infty}K_{5/3}(u)\,{\rm d}u$ should be replaced by $\frac{\nu}{\nu_c}\int_{\nu/\nu_c}^{\infty}K_{5/3}(u)\,{\rm d}u$.

The calculation of the absorption coefficient for circular polarization in equation (84) is less straightforward because its dominant order contribution involves the integral of an odd function of ϖ, or ψ, which vanishes. Thus, K_{IV}/c generically is much smaller than the other two absorption coefficients. Using Nicholson's approximation for $J_\sigma(x)$ and $J'_\sigma(x)$, equation (84) becomes

$$\frac{K_{IV}}{c} = -\frac{4\sqrt{2}}{3}\,s_q\,\frac{\omega_{pr}^2\Omega^2}{c\,\omega^3}\iint u^2\,m^3c^3\sin\vartheta\sqrt{\gamma^2-1}\,{\rm d}\gamma\,{\rm d}\psi\;\frac{\partial F_0}{\partial\sigma}\;\varpi\;\frac{(\sigma-x)^{3/2}}{x^{1/2}}\;K_{1/3}(g)K_{2/3}(g). \tag{104}$$

The integrand on the right-hand side of equation (104) should be expressed in terms of γ and ϑ from equation (A1) and expanded to the first non-vanishing even order in ψ. This implies that the angle derivative term in $\partial_\sigma F_0$ (equation A6), which is of order ψ, should be accounted for, that the derivative $\partial_\gamma F_0$ be Taylor-expanded about $\vartheta=\alpha$ and that all other factors involved in equation (104) be similarly expanded. This applies in particular to the product of Bessel functions, owing to the fact that the actual value of their argument g, given by equation (94), slightly differs from its lowest order approximation in ψ. With two terms, this argument g may actually be expanded as

$$g = g_0 + g_1 = \frac{\gamma u}{3\,\sin\alpha}\left(\psi^2+\frac{1}{\gamma^2}\right)^{3/2} - \frac{\gamma u\cos\alpha}{6\sin^2\alpha}\,\psi\left(\psi^2+\frac{1}{\gamma^2}\right)^{3/2}. \tag{105}$$

Integrating the correction to the product of Bessel functions over ψ by parts, these expansions lead to

$$\begin{aligned}\frac{K_{IV}}{c} &= -\frac{2}{3}s_q\frac{\omega_{\rm pr}^2}{c\,|\,\Omega\,|}\iint\frac{m^3c^3}{\sin\alpha}\,\gamma^3\,{\rm d}\gamma\,{\rm d}\psi\;\frac{\partial F_0}{\partial\gamma}\;\frac{\cos\alpha}{\sin\alpha}\left(2\psi^2+\frac{2}{3\gamma^2}\right)\left(\psi^2+\frac{1}{\gamma^2}\right)^{3/2}K_{1/3}(g_0)K_{2/3}(g_0)\,,\\ &\quad -\frac{2}{3}s_q\frac{\omega_{\rm pr}^2}{c\,|\,\Omega\,|}\iint\frac{m^3c^3}{\sin\alpha}\,\gamma^3\,{\rm d}\gamma\,{\rm d}\psi\;\left(\frac{\partial^2F_0}{\partial\gamma\,\partial\vartheta}-\frac{1}{\gamma}\frac{\partial F_0}{\partial\vartheta}\right)\psi^2\left(\psi^2+\frac{1}{\gamma^2}\right)^{3/2}K_{1/3}(g_0)K_{2/3}(g_0),\end{aligned} \tag{106}$$

where, again, all derivatives of F_0 are to be taken at $\vartheta=\alpha$. The integration over ψ is carried out following a procedure similar to that described by Westfold (1959), which gives

$$\begin{aligned}\frac{K_{IV}}{c} &= -\frac{2\pi}{\sqrt{3}}s_q\frac{\omega_{\rm pr}^2\,|\,\Omega\,|}{c\,\omega^2}\,\cos\alpha\int m^3c^3\gamma\,{\rm d}\gamma\;\frac{\partial F_0}{\partial\gamma}\;\left(\int_{\frac{\omega}{\omega_c}}^{\infty}K_{1/3}(u)\,{\rm d}u+\frac{\omega}{\omega_c}K_{1/3}\left(\frac{\omega}{\omega_c}\right)\right)\\ &\quad -\frac{\pi}{\sqrt{3}}s_q\frac{\omega_{\rm pr}^2\,|\,\Omega\,|}{c\,\omega^2}\,\sin\alpha\int m^3c^3\gamma\,{\rm d}\gamma\;\left(\frac{\partial^2F_0}{\partial\gamma\,\partial\vartheta}-\frac{1}{\gamma}\frac{\partial F_0}{\partial\vartheta}\right)\int_{\frac{\omega}{\omega_c}}^{\infty}K_{1/3}(u)\,{\rm d}u.\end{aligned} \tag{107}$$

The result in equation (107) coincides with that given by Sazonov (1969a) in his equation 2.2.

5.3 NR contribution to transfer coefficients from Debye's expansion

In the NR regime, the variable g of equation (94) is larger than unity. The variables x and σ both remain large but need not be almost equal. These conditions are suitable for using the Debye expansion of Bessel functions of large indices and argument (Watson 1922; Matviyenko

1992), subject to the condition that $(\sigma - x) \gg \sigma^{1/3}$ and, in our case, that $x < \sigma$. The Debye expansion represents the Bessel functions of large index σ for a given value of the argument-to-index ratio x/σ, represented by a parameter ξ such that

$$\frac{x}{\sigma} = \frac{1}{\cosh\xi}. \tag{108}$$

The Debye expansions of $J_\sigma(x)$ and $N_\sigma(x)$ can be written as (Watson 1922)

$$J_\sigma(x) \equiv J_\sigma\left(\frac{\sigma}{\cosh\xi}\right) = +\frac{\mathrm{e}^{\sigma(\tanh\xi-\xi)}}{\sqrt{2\pi\sigma\tanh\xi}}\ \sum_{m=0}^{\infty}\frac{\Gamma(m+1/2)}{\Gamma(1/2)}\ \frac{2^m\ A_m(\xi)}{(\sigma\tanh\xi)^m}, \tag{109}$$

$$N_\sigma(x) \equiv N_\sigma\left(\frac{\sigma}{\cosh\xi}\right) = -\frac{\sqrt{2}\,\mathrm{e}^{\sigma(\xi-\tanh\xi)}}{\sqrt{2\pi\sigma\tanh\xi}}\ \sum_{m=0}^{\infty}\frac{\Gamma(m+1/2)}{\Gamma(1/2)}\ \frac{(-1)^m\,2^m\ A_m(\xi)}{(\sigma\tanh\xi)^m}, \tag{110}$$

where the coefficients A_m depend on ξ, but for A_0 that equals unity. $\Gamma(y)$ denotes the gamma function of argument y. The nth term in the sum is of order σ^{-n}, that is of order $(|\Omega|/\omega)^n$. Here we only need to proceed to second order. It can be checked that at this order the Debye approximation continuously merges into Nicholson's approximation at their common limit of validity. While σ is regarded as a large parameter in the expansions in equations (109) and (110), the ratio x/σ should be considered of order unity. Approximations to $J'_\sigma(x)$ and $N'_\sigma(x)$ are obtained by differentiating equations (109) and (110) with respect to x at fixed σ, taking care of the fact that the auxiliary variable ξ depends on x, and thus also the coefficients A_1 and A_2. Some terms resulting from this differentiation contribute at this order. All calculations done, we obtain

$$J_\sigma(x)N_\sigma(x) = \frac{(-1)}{\pi\sqrt{\sigma^2-x^2}}\ \left(1+\frac{6A_2-A_1^2}{\sigma^2-x^2}\right), \tag{111}$$

$$J'_\sigma(x)N_\sigma(x) = \frac{(-1)}{\pi x}\left(1+\frac{1}{2}\,\frac{x^2}{(\sigma^2-x^2)^{3/2}}+\frac{6A_2+xA'_1-A_1^2}{\sigma^2-x^2}+\frac{3}{2}\,\frac{A_1x^2}{(\sigma^2-x^2)^2}\right), \tag{112}$$

$$J'_\sigma(x)N'_\sigma(x) = \frac{\sqrt{\sigma^2-x^2}}{\pi x^2}\ \left(1+\frac{6A_2+2xA'_1}{\sigma^2-x^2}+\frac{2A_1\,x^2}{(\sigma^2-x^2)^2}-\frac{A_1^2}{\sigma^2-x^2}-\frac{1}{4}\,\frac{x^4}{(\sigma^2-x^2)^3}\right), \tag{113}$$

where

$$A_1 = \frac{1}{8}-\frac{5}{24}\,\frac{\sigma^2}{\sigma^2-x^2}\,, \qquad A_2 = \frac{3}{128}-\frac{77}{576}\,\frac{\sigma^2}{\sigma^2-x^2}+\frac{385}{3456}\,\frac{\sigma^4}{(\sigma^2-x^2)^2}\,, \qquad xA'_1 = -\frac{5}{12}\,\frac{\sigma^2x^2}{(\sigma^2-x^2)^2}. \tag{114}$$

The first terms in the parentheses of equations (111)–(113), that are equal to unity, remain in the unmagnetized limit, $\Omega \to 0$. The non-Bessel terms in equations (86) and (87) are comparable to them. The NR contributions to equations (88) and (89) are obtained by integrating these expansions of the Bessel functions over the NR domain, denoted by the suffix NR:

$$f_{\rm NR} = \frac{2\pi^2 s_q}{c}\,\frac{\omega_{\rm pr}^2\Omega^2}{\omega^3}\iint_{\rm NR}\frac{m^3c^3}{\sin^2\alpha}\,\mathrm{d}\varpi\,\mathrm{d}\sigma\ \ \frac{\varpi}{\pi}\,\frac{\partial F_0}{\partial\sigma}\ \left(\frac{1}{2}\,\frac{x^2}{(\sigma^2-x^2)^{3/2}}+\frac{6A_2+xA'_1-A_1^2}{\sigma^2-x^2}+\frac{3}{2}\,\frac{A_1x^2}{(\sigma^2-x^2)^2}\right), \tag{115}$$

$$\begin{aligned} h_{\rm NR} = {} & \frac{\pi^2\omega_{\rm pr}^2\Omega^2}{c\,\omega^3}\iint_{\rm NR}\frac{m^3c^3}{\sin^2\alpha}\,\mathrm{d}\varpi\,\mathrm{d}\sigma\ \frac{\partial F_0}{\partial\sigma}\ \frac{2\sqrt{\sigma^2-x^2}}{\pi}\ \left(1+\frac{6A_2-A_1^2+xA'_1}{\sigma^2-x^2}+\frac{A_1x^2}{(\sigma^2-x^2)^2}-\frac{1}{8}\,\frac{x^4}{(\sigma^2-x^2)^3}\right)\\ & -\frac{\pi^2\omega_{\rm pr}^2\Omega^2}{c\,\omega^3}\iint_{\rm NR}\frac{m^3c^3}{\sin^2\alpha}\,\mathrm{d}\varpi\,\mathrm{d}\sigma\ \frac{\partial F_0}{\partial\sigma}\ \frac{\sigma_0^2}{\pi\sqrt{\sigma^2-x^2}}\left(1+\frac{6A_2-A_1^2}{\sigma^2-x^2}\right)+\frac{\pi\omega_{\rm pr}^2\Omega^2}{c\,\omega^3}\int_{-\infty}^{+\infty}\frac{m^3c^3}{\sin^2\alpha}\,\mathrm{d}\varpi\ \frac{2\varpi^2+\sigma_0^2}{\sqrt{\varpi^2+\sigma_0^2}}\,F_0(\varpi,\sigma_b(\varpi)). \end{aligned} \tag{116}$$

It is remarkable that the terms independent of magnetization eventually disappeared from equation (115). They also cancel out in equation (116) as we now show. Gathering and arranging them, these terms can be written as

$$h_{\rm NR}^{(0)} = \frac{\pi\omega_{\rm pr}^2\Omega^2}{c\,\omega^3}\iint_{\rm NR}\frac{m^3c^3}{\sin^2\alpha}\,\mathrm{d}\varpi\,\mathrm{d}\sigma\ \frac{\partial F_0}{\partial\sigma}\,\frac{2\varpi^2+\sigma_0^2}{\sqrt{\varpi^2+\sigma_0^2}}+\ \frac{\pi\omega_{\rm pr}^2\Omega^2}{c\,\omega^3}\int_{-\infty}^{+\infty}\frac{m^3c^3}{\sin^2\alpha}\,\mathrm{d}\varpi\ \frac{2\varpi^2+\sigma_0^2}{\sqrt{\varpi^2+\sigma_0^2}}\,F_0(\varpi,\sigma_b(\varpi)). \tag{117}$$

The double integral term may be integrated explicitly over σ at given ϖ since only $\partial_\sigma F_0$ depends on this variable. The integration is on the values of σ between its value $\sigma_b(\varpi)$ on the boundary $\mathcal{B}$ of the physical domain and its value $\sigma_{\rm QR}(\varpi) = (\varpi^2+\sigma_0^2)^{3/4}/\sqrt{3}$ on the boundary $\mathcal{B}_{\rm QR}$ between the NR and QR domains. The contribution from the lower boundary, $\sigma_b(\varpi)$, cancels the term that was already in the form of a single integral over ϖ. The contribution from the upper boundary at $\sigma_{\rm QR}(\varpi)$ remains and could as well be considered to be part of the QR contribution since it can be written as an integral over the QR domain. Naming this contribution $h_{\rm BQR}$:

$$h_{\rm BQR} = \frac{\pi\omega_{\rm pr}^2\Omega^2}{c\,\omega^3}\int_{-\infty}^{+\infty}\frac{m^3c^3}{\sin^2\alpha}\,\mathrm{d}\varpi\ \frac{2\varpi^2+\sigma_0^2}{\sqrt{\varpi^2+\sigma_0^2}}\,F_0(\varpi,\sigma_{\rm BQR}(\varpi)) = -\frac{\pi\omega_{\rm pr}^2\Omega^2}{c\,\omega^3}\iint_{\rm QR}\frac{m^3c^3}{\sin^2\alpha}\,\mathrm{d}\varpi\,\mathrm{d}\sigma\ \frac{2\varpi^2+\sigma_0^2}{\sqrt{\varpi^2+\sigma_0^2}}\,\frac{\partial F_0}{\partial\sigma}. \tag{118}$$

We refer to the remainder of the NR contribution to h as the reduced NR contribution $\hat{h}_{\rm NR}$:

$$\hat{h}_{\rm NR} = \pi \frac{\omega_{\rm pr}^2 \Omega^2}{c\,\omega^3} \iint_{\rm NR} \frac{m^3c^3}{\sin^2\alpha}\,{\rm d}\varpi\,{\rm d}\sigma \left(2\left(\frac{6A_2 - A_1^2 + xA_1'}{(\sigma^2-x^2)^{1/2}} + \frac{A_1 x^2}{(\sigma^2-x^2)^{3/2}} - \frac{1}{8}\,\frac{x^4}{(\sigma^2-x^2)^{5/2}} \right) - \sigma_0^2 \left(\frac{6A_2 - A_1^2}{(\sigma^2-x^2)^{3/2}} \right) \right) \frac{\partial F_0}{\partial \sigma}. \tag{119}$$

The $\mathcal{B}_{\rm QR}$ contribution to h in equation (118) is then associated with the QR contribution $h_{\rm QR}$ in equation (100) to form a reduced QR contribution $\hat{h}_{\rm QR}$:

$$\hat{h}_{\rm QR} = \frac{\omega_{\rm pr}^2 \Omega^2}{c\,\omega^3} \iint_{\rm QR} \frac{m^3c^3}{\sin^2\alpha}\,{\rm d}\varpi\,{\rm d}\sigma \left(\frac{4x^2}{\sqrt{3}} \left(\frac{\sigma - x}{x} \right)^2 K_{\frac{2}{3}}(g) L_{\frac{2}{3}}(g) + \frac{2\varpi^2}{\sqrt{3}} \left(\frac{\sigma - x}{x} \right) K_{\frac{1}{3}}(g) L_{\frac{1}{3}}(g) - \pi \frac{2\varpi^2 + \sigma_0^2}{\sqrt{\varpi^2 + \sigma_0^2}} \right) \frac{\partial F_0}{\partial \sigma}. \tag{120}$$

The combinations of the functions A_1, A_2 and xA_1' that appear in equations (115) and (119) may be expressed in terms of σ and x by using equation (114). When the integration over the NR domain can be extended to the full domain, this results in equations (28) and (29).

5.4 NR versus QR contribution to the Faraday coefficients

The QR contributions to the Faraday coefficients are given by equations (99) and (120) and the NR ones by equations (115) and (119). We now compare them, making a simple ansatz concerning the distribution function, namely that F_0 is a linear function of ϖ, so that $\partial_\sigma F_0 = F_{0\sigma}(\sigma) + \varpi F_{0\sigma\varpi}(\sigma)$. The $F_{0\sigma}$ term produces a nil contribution to f if, as assumed here, it depends on σ alone. The $\varpi F_{0\sigma\varpi}$ term produces a vanishing contribution to h since its kernel is an even function of ϖ. This ansatz is sufficient to give a hint on the dependence of the transfer coefficients on the distribution function. The contributions $f_{\rm NR}$ and $f_{\rm QR}$ to f, or $h_{\rm NR}$ and $h_{\rm QR}$ to h, may then be written in a form involving a kernel depending on σ, such that

$$f_{\rm R} = 2s_q \frac{\omega_{\rm pr}^2 \Omega^2}{c\,\omega^3} \int_{\rm R} \frac{m^3c^3}{\sin^2\alpha}\,{\rm d}\sigma\; K_{\rm R}^{(f)}(\sigma) F_{0\sigma\varpi}(\sigma)\,, \qquad\qquad h_{\rm R} = \frac{\omega_{\rm pr}^2 \Omega^2}{c\,\omega^3} \int_{\rm R} \frac{m^3c^3}{\sin^2\alpha}\,{\rm d}\sigma\; K_{\rm R}^{(h)}(\sigma) F_{0\sigma}(\sigma), \tag{121}$$

where R stands either for the QR or NR domain and $K_{\rm R}^{(f)}(\sigma)$ and $K_{\rm R}^{(h)}(\sigma)$ are corresponding one-variable kernels, integrated over ϖ at given σ. For Faraday rotation,

$$K_{\rm NR}^{(f)}(\sigma) = \int_{\rm NR} {\rm d}\varpi\; \frac{\pi}{2}\,\frac{\varpi^2 x^2}{(\sigma^2-x^2)^{3/2}}\,, \qquad\qquad K_{\rm QR}^{(f)}(\sigma) = \int_{\rm QR} {\rm d}\varpi\; \frac{2^{3/2}}{3^{1/2}}\,\varpi^2 x \left(\frac{\sigma - x}{x} \right)^{3/2} \left(K_{2/3}(g) L_{1/3}(g) - \frac{\pi}{\sqrt{3}\,g} \right). \tag{122}$$

The QR kernel for f, on the right of equation (122), can be expressed in terms of the variable g from equation (H4) and then be integrated over the QR domain $g_m(\sigma) < g < 1$. The lower bound g_m, defined in equation (H4), approaches zero when σ diverges. The integral on the right of equation (122) converges as g_m approaches zero, which it does when σ grows much larger than $\sigma_{\rm QR}$. The asymptotic NR part of the kernel of f can be calculated as shown in Appendix H. The results, valid for $\sigma \gg \sigma_{\rm QR}$, are

$$K_{\rm NR}^{(f)}(\sigma) \approx \frac{\pi}{3}\,\sigma^2\,\ln\left(\frac{\sigma}{3}\right), \qquad\qquad K_{\rm QR}^{(f)}(\sigma) \approx 0.6\,\sigma^2. \tag{123}$$

The NR contribution to f slightly dominates when $\sigma \gg \sigma_{\rm QR}$. These results partly depend on our assumption that the distribution function depends linearly on ϖ. Otherwise, $f_{\rm NR}$ would also have a term proportional to $F_{0\sigma}$ that is absent from equation (121) by imparity. We return to this in Section 6.3.

The ϖ-integrated kernel for h being defined as in equation (121), its NR part results from equation (119) and is calculated in Appendix H. The QR part $\hat{h}_{\rm QR}$ is given by equation (120) and its calculation is also outlined in this appendix. The kernels $K_{\rm NR}^{(h)}(\sigma)$ and $K_{\rm QR}^{(h)}(\sigma)$ turn out to be approximately given, for $\sigma \gg \sigma_{\rm QR}$ by

$$K_{\rm NR}^{(h)}(\sigma) \approx -\frac{\pi}{8}\left(\frac{\sigma}{3}\right)^{4/3}, \qquad\qquad K_{\rm QR}^{(h)}(\sigma) \approx +\frac{\pi}{2}\,\sigma^{4/3}. \tag{124}$$

A glance at equation (124) shows that both contributions to the kernel $K^{(h)}$ vary when $\sigma \gg \sigma_{\rm QR}$ as $\sigma^{4/3}$, the QR one being numerically larger.

The scaling in $\sigma^{4/3}$ anticipated for the h kernel from equation (124) does not conflict with the fact that the Faraday conversion coefficient h decreases to zero at high temperature for thermal distributions (Huang & Shcherbakov 2011). We have confirmed this decline of $h^{\rm th}$ with temperature by numerically integrating equation (89) for a thermal distribution function and checked its compatibility with a kernel in $\gamma^{4/3}$. We return to this in Section 6.2. The Faraday conversion coefficient h is largely affected by the QR contribution to it, which is of an opposite sign to the NR one. Equations (31) and (32) propose a simple, though crude, way to account for the increasing importance of the QR contribution which should be good enough wherever the balance passes from NR to QR domination. For a given ω, the QR domain becomes narrower in angle as γ increases and the QR kernel has an effectively compact support in this domain. Therefore, our calculation in equation (124) of the QR contribution to h should be close to being exact at large γ's, since $\partial F_0/\partial\sigma$ certainly is almost constant with ϖ over the narrow QR domain, as was assumed in this section.

The condition for the QR domain not to contribute to the transfer coefficients is that the distribution function be negligible in it. From equation (92), this happens when for most particles $\sigma - \sqrt{\sigma^2 - \sigma_0^2} > \sigma^{1/3}$, or equivalently when the variable g in equation (94) is larger than unity. Expanding the expression of the latter condition in σ_0/σ and noting that $\sigma = \gamma u \sin^2\alpha$ at $\varpi = 0$, this inequality reduces again to the condition that equation (27) be satisfied. Up to a somewhat arbitrary factor, the parameter on the left of equation (27) is similar to the square of the regime-change parameters X and $\gamma_0 X_A$, respectively, defined by Shcherbakov (2008) and Huang & Shcherbakov (2011). When

the inequality in equation (27) is not satisfied, the coefficients f and h differ from their HF approximations in equations (145) and (146) below, where the integration is meant to extend over the full ϖ–σ domain. The intrusion of QR contributions is at the origin of the change in the trend of the variations of f and h with temperature described by Shcherbakov (2008) for thermal distributions. This author attributes this change to a failure of the HF expansion, which is correct in the sense that the QR contribution cannot be expressed in the form of a series expansion, no partial sum of the Debye series being able to represent the Bessel function in the domain of validity of Nicholson's approximation.

6 LF KERNELS OF FARADAY COEFFICIENTS OF ISOTROPIC DISTRIBUTIONS

6.1 Remarks on the LF limit of isotropic kernels for the Faraday coefficients

In the limit of large γ's, the QR domain contributes little to the Faraday rotation coefficient f, given by equation (88), because it involves the integral of an odd function of the difference $\psi = \vartheta - \alpha$ on the small QR domain. This remark holds also for the integral over the same QR domain of the NR contribution. For an isotropic distribution, there is however a non-vanishing NR contribution to f that is proportional to $\partial_\gamma F_0$. Such a contribution is absent for distributions, as considered in Section 5.4, that are linear in ϖ.

By contrast, the QR domain, if substantially populated with particles, largely contributes the Faraday conversion coefficient h. Particles in the QR domain satisfy the inequality inverse to that in equation (27) in a strong sense. We refer to the case when this strong inequality is satisfied as the LF limit. Since any isotropic distribution function depends on γ only, the Faraday coefficients for such distributions can be reduced to a single quadrature over the Lorentz factor involving a γ-dependent kernel as defined in equation (33). The exact expression of the isotropic kernel for f results from equation (88) in which the variables ϖ–σ should be changed to ϖ–γ, giving on integrating over ϖ at a given γ

$$F^{\rm iso}(\gamma) = -\frac{2\pi^2 s_q}{\sin^2\alpha}\int_{\varpi_-}^{\varpi_+} {\rm d}\varpi\ \varpi\, x\left(J'_\sigma(x)N_\sigma(x) + \frac{1}{\pi x}\right). \tag{125}$$

The exact isotropic kernel for h is similarly obtained from equation (87), in which the principal value term should be neglected. Using equations (A1)–(A7), the isotropic kernel for h can be written as

$$H^{\rm iso}(\gamma) = \frac{\pi^2}{\sin^2\alpha}\int_{\varpi_-}^{\varpi_+} {\rm d}\varpi\left(x^2 J'_\sigma(x)N'_\sigma(x) - \varpi^2 J_\sigma(x)N_\sigma(x) - \frac{1}{\pi}\left(\gamma u \sin^2\alpha + 2\varpi\cos\alpha\right)\right). \tag{126}$$

In equations (125) and (126), the bounds $\varpi_\pm(\gamma)$ are defined by equation (37). The kernel $H^{\rm iso}(\gamma)$ could have been deduced as well from equation (89), reformulating the line-integral term in it as a surface integral. These different expressions are equivalent because the non-Bessel integrals in them, though apparently different, are actually equal, given the particular values of the bounds.

6.2 Thermal Faraday conversion coefficient in the LF limit

To check the behaviour of the Faraday conversion coefficient h in the LF limit, we have numerically integrated its quasi-exact expression in equation (126) with `Mathematica` for a thermal distribution function. At a given frequency, the LF limit would then correspond to the limit of high temperatures. Huang & Shcherbakov (2011) have found that in this limit the Faraday conversion coefficient decreases with temperature. We confirm this and find that this decrease scales as $-T^{-5/3}$ by extending our numerical calculations to high values of the temperature T (see Fig. 2). This has been possible by using the uniform expansion for high-order Bessel functions derived by Olver (1954) which allows a fast and reliable calculation of high-order Bessel functions (see Appendix G). Returning the result of the integration over the directions of the particles before performing that over γ reveals the high-energy properties of the isotropic kernels derived in Sections 6.3 and 6.4. This numerically supports the analytical result, reached in Section 6.4 and shown in Fig. 7, that the kernel of h asymptotically grows with

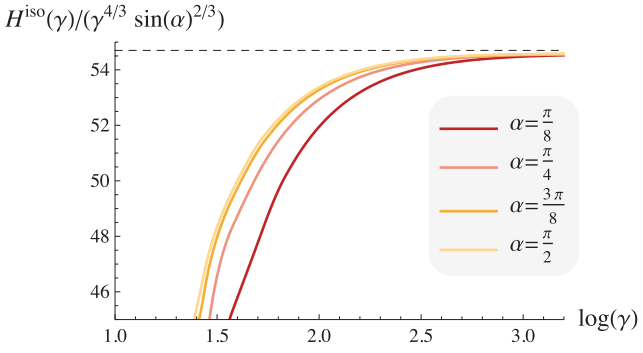

Figure 7. The evolution of $H^{\rm iso}(\gamma)/(\gamma^{4/3}\sin^{2/3}\alpha)$ [computed via equation (126) using the Olver expansion] as a function of γ for different values of α. The radiation's parameter $u = 15$. For all values of α, this ratio asymptotes to a constant for large γ. The dashed line corresponds to the asymptotic prediction of equation (138).

the Lorentz factor as $\gamma^{4/3}$ and shows that this increase with energy of the kernel is consistent with the fast decline with temperature of the thermal Faraday conversion coefficient. Note finally that, considering equations (42) and (33), equation (138) predicts at large γ the result of the numerical integration and the $T^{-5/3}$ asymptote for the thermal distribution.

6.3 Isotropic kernel of the Faraday rotation coefficient in the LF limit

The integral in equation (125) may be separated into NR and QR parts as follows. The Faraday rotation kernel $F^{\rm iso}(\gamma)$ is the sum of the expression in equation (115), integrated over the NR domain and limited to its lowest order term in Ω/ω, and of the QR contribution from equation (99). The integral over the NR domain in equation (115) can be extended to the full domain at the expense of adding, if needed, to the contribution from equation (99) a correction to account for the undue integration over the QR domain so introduced. After the necessary change of variables, and considering the result in equation (38), the kernel $F^{\rm iso}(\gamma)$ assumes the, still exact, form

$$F^{\rm iso}(\gamma) = 4\pi s_q \frac{\omega\cos\alpha}{|\Omega|}\left(\gamma\,\mathcal{L}(\gamma) - \sqrt{\gamma^2-1}\right) - \pi s_q \frac{\Theta_H(\gamma-\gamma_{\rm QR})}{\sin^2\alpha}\int_{\rm QR} {\rm d}\varpi\ \frac{\varpi\, x^2}{(\sigma^2-x^2)^{3/2}}$$
$$+ 2 s_q \frac{\Theta_H(\gamma-\gamma_{\rm QR})}{\sin^2\alpha}\int_{\rm QR} {\rm d}\varpi\ \varpi\left(\sqrt{3} g K_{2/3}(g) L_{1/3}(g) - \pi\right). \tag{127}$$

The first term in the first line of equation (127) is the NR isotropic kernel, calculated by integration over the full physical domain. The second term in the first line is an integral at given γ over the QR domain correcting for the fact that the NR domain really does not extend over the full physical one. The second line is the QR contribution proper. The variables σ, x and g are functions of γ and ϖ that may be found from Appendix A and equation (94). The QR integration over ϖ is between $\varpi_{\rm QR-}$ and $\varpi_{\rm QR+}$ defined in the caption of Fig. 6.

As γ approaches infinity, the interval $[\varpi_{\rm QR-},\ \varpi_{\rm QR+}]$ becomes more and more symmetrical about zero while $g(+\varpi,\ \gamma)$ and $g(-\varpi,\ \gamma)$ converge to each other. The second and third terms in equation (127) then approach the integral of an odd function over an interval symmetrical with respect to $\varpi = 0$, which then vanishes. As for the circular polarization absorption coefficient K_{IV} calculated in Section 5.2, higher order terms determine the QR contribution. Since only isotropic distributions are considered in this section, corrections caused by the anisotropy of the distribution function are absent. However, the interval $[\varpi_{\rm QR-},\ \varpi_{\rm QR+}]$ is slightly asymmetrical with respect to $\varpi = 0$, which gives rise to a first-order 'offset' correction. Moreover, $\sigma(+\varpi,\ \gamma)$ and $\sigma(-\varpi,\ \gamma)$ slightly differ when $\varpi \ll \gamma u \sin^2\alpha$, as can be seen from equation (A1), and then $g(+\varpi,\ \gamma)$ and $g(-\varpi,\ \gamma)$ differ by the quantity g_1 in equation (105). Thus, the integrands in the QR integrals in equation (127) have a small even part that gives rise to a 'parity' correction to these integrals. At large γ's, the offset $\Delta\varpi_{\rm QR}$ is given by the expansions in equations (J2) and (J3), eventually giving for the offset correction (Appendix K)

$$F^{\rm iso}_{\rm off}(\gamma) = -\frac{4\pi\, s_q}{3}\,\gamma u\cos\alpha + 8 s_q \gamma u\cos\alpha\,\left(\sqrt{3} K_{2/3}(1) L_{1/3}(1) - \pi\right). \tag{128}$$

The parity corrections are evaluated by integrating the even part of the integrands in equation (127) over the symmetric interval $[-3^{1/3}(\gamma u\sin^2\alpha)^{2/3}, +3^{1/3}(\gamma u\sin^2\alpha)^{2/3}]$. The even part of the integrand in the second line of equation (127) is obtained by Taylor-expanding in g the function in the parentheses about g_0 as in equation (105), then performing the integration by using g as the integration variable. To sufficient accuracy, g is related to ϖ by the lowest order relation in equation (J6). The minimum value g_m of g, reached at $\varpi = 0$, is given by equation (H4) and approaches zero as γ grows larger. The parity correction from the second line of equation (127) is thus evaluated taking $g_m = 0$. The calculation of the parity correction from the first line is more straightforward. All calculations done (Appendix K), it is found that

$$F^{\rm iso}_{\rm par}(\gamma) = -\pi s_q \gamma u\cos\alpha\left[\frac{8}{3}\ln(\gamma) + \frac{4}{3}\ln\left(\frac{\sin\alpha}{u}\right) + 2\ln(4) + \frac{4}{3}\ln(3) - 4 + \frac{8\sqrt{3}}{\pi}\int_0^1 {\rm d}g\, g\frac{\rm d}{{\rm d}g}\left(\sqrt{3} g K_{2/3}(g) L_{1/3}(g)\right)\right]. \tag{129}$$

An asymptotic expansion of $F^{\rm iso}$ for large γ's is finally obtained by expanding the first term of equation (127) up to order γ, integrating by parts the last term of equation (129), which partly simplifies with the second term of equation (128), and numerically calculating the coefficients of the terms of the expansion. This gives

$$F^{\rm iso}_{\rm LF}(\gamma) = \pi s_q\,\gamma\, u\cos\alpha\left(\frac{4}{3}\ln\left(\frac{\gamma u}{\sin\alpha}\right) - 1.260\,724\,39\right). \tag{130}$$

6.4 Isotropic kernel of the Faraday conversion coefficient in the LF limit

The integral in equation (126) can be separated into an NR and a QR contribution. This is best achieved by writing the kernel $H^{\rm iso}(\gamma)$ as the sum of the contributions to it from equations (119) and (120), which may be modified by extending the former integral to the full σ–ϖ domain and adding to equation (120) a correction to account for the undue integration over the QR domain so introduced. The variables are then changed to γ and ϖ. The extended NR contribution then provides the result in equation (39) while the expression for the correction to the QR contribution is similar to that in equation (35), the boundaries of the integral over ϖ being however placed at $\varpi_{\rm QR+}(\gamma)$ and $\varpi_{\rm QR-}(\gamma)$

on the edge of the QR domain shown in Fig. 6. The kernel $H^{\rm iso}(\gamma)$ then takes the form

$$H^{\rm iso}(\gamma) = -\frac{\pi}{2}\,\sin^2\!\alpha\,\left(\gamma\,(2\gamma^2-3)\,\sqrt{\gamma^2-1}+\mathcal{L}(\gamma)\right)+\frac{\Theta_H(\gamma-\gamma_{\rm QR})}{\sin^2\alpha}\int_{\varpi_{\rm QR-}}^{\varpi_{\rm QR+}}{\rm d}\varpi\;\frac{\pi}{8}\left(\frac{2x^4}{(\sigma^2-x^2)^{5/2}}+\sigma_0^2\,\frac{x^2(4\sigma^2+x^2)}{(\sigma^2-x^2)^{7/2}}\right)$$

$$+\frac{\Theta_H(\gamma-\gamma_{\rm QR})}{\sin^2\alpha}\int_{\varpi_{\rm QR-}}^{\varpi_{\rm QR+}}{\rm d}\varpi\;\left(\frac{4x^2}{\sqrt{3}}\left(\frac{\sigma-x}{x}\right)^2K_{2/3}(g)L_{2/3}(g)+\frac{2\varpi^2}{\sqrt{3}}\left(\frac{\sigma-x}{x}\right)K_{1/3}(g)L_{1/3}(g)-\pi\,\frac{2\varpi^2+\sigma_0^2}{\sqrt{\varpi^2+\sigma_0^2}}\right)\,. \tag{131}$$

The first term in the first line of equation (131) is the NR isotropic kernel, calculated by integration over the full physical domain. The second term in the first line is an integral over the QR domain correcting for the fact that the NR domain really does not extend over the full physical one. The second line is the QR contribution proper. The LF limit of this kernel is to be obtained from an asymptotic expansion in γ on the right-hand side of equation (131). This LF development is valid when $\gamma \gg \gamma_{\rm QR} \approx (u/(3\sin\alpha))^{1/2}$. The domain of validity of the LF limit is where $\omega \ll 3\gamma^2\sin\alpha|\Omega|$ (equation 27), which is equivalent to $\omega \ll \omega_c(\gamma,\alpha)$, where ω_c is the characteristic frequency of synchrotron emission defined in equation (101).

As discussed in Section 5.1, the variable g in equation (94) is less than unity in the QR domain. At the order required by the calculations in this subsection, the lowest order approximation to the values of $\varpi_{\rm QR\pm}(\gamma)$ is sufficient, namely

$$\varpi_{\rm QR\pm}(\gamma) \approx \pm\left(3\gamma^2u^2\sin^4\!\alpha\right)^{1/3}\,. \tag{132}$$

From equations (A1) and (A2), the integrand in the first line of equation (131) can be written in terms of ϖ and γ, or $G=\gamma u\sin^2\!\alpha/3$, as

$$\frac{2x^4}{(\sigma^2-x^2)^{5/2}}+\sigma_0^2\,\frac{x^2(4\sigma^2+x^2)}{(\sigma^2-x^2)^{7/2}} = \frac{162G^4}{(\varpi^2+\sigma_0^2)^{5/2}}\left(1+\frac{2\varpi\cos\alpha}{3G}-\frac{\varpi^2\sin^2\!\alpha+\sigma_0^2}{9G^2}\right)^2$$

$$+\frac{405\sigma_0^2G^4}{(\varpi^2+\sigma_0^2)^{7/2}}\left(1+\frac{2\varpi\cos\alpha}{3G}-\frac{\varpi^2\sin^2\!\alpha+\sigma_0^2}{9G^2}\right)\left(1+\frac{2\varpi\cos\alpha}{3G}+\frac{5\varpi^2\cos^2\!\alpha-\varpi^2-\sigma_0^2}{45G^2}\right)\,. \tag{133}$$

The primitive of this function is shown in Appendix J. The integral over ϖ that appears in the second term of the first line of equation (131) can be obtained from it and expanded to the required order in γ. It is inferred from Section 5.4 that this order should be $\mathcal{O}(\gamma^{4/3})$. The expansion procedure, outlined in Appendix J, leads to

$$\frac{\pi}{8\sin^2\alpha}\int_{\varpi_{\rm QR-}}^{\varpi_{\rm QR+}}{\rm d}\varpi\;\left(\frac{2x^4}{(\sigma^2-x^2)^{5/2}}+\sigma_0^2\,\frac{x^2(4\sigma^2+x^2)}{(\sigma^2-x^2)^{7/2}}\right) \;\approx\; \pi\sin^2\!\alpha\,\gamma^4-2\pi\sin^2\!\alpha\,\gamma^2-\frac{\pi}{8}\,\sin^{2/3}\!\alpha\,\left(\frac{\gamma u}{3}\right)^{4/3}\,. \tag{134}$$

The proper QR contribution to $H^{\rm iso}(\gamma)$ originates from the integration over ϖ in the second line in equation (131). This contribution is calculated to order $\gamma^{4/3}$ by changing the variable ϖ for the variable g on which the K and L functions depend, much as was done in Section 5.4, but for the fact that the integration over ϖ is now performed at constant γ instead of at constant σ. Some details are presented in Appendix J. From these calculations it is found that the LF limit to the QR contribution to the kernel $H^{\rm iso}(\gamma)$ is

$$H^{\rm iso}_{\rm QR}(\gamma) = 2\,(\gamma u)^{4/3}\,(\sin\alpha)^{2/3}\;3^{1/6}\int_0^1{\rm d}g\;g^{2/3}\left(K_{2/3}(g)L_{2/3}(g)+K_{1/3}(g)L_{1/3}(g)-\frac{2\pi}{\sqrt{3}\,g}\right)\,. \tag{135}$$

The integrand in equation (135) declines rapidly to zero out of the QR domain (see Section 5.4) and the value of the definite integral over g is, with a relative error of only 10^{-4}, equal to $\pi/(4\,\times\,3^{1/6})$. Adopting this value, we eventually get

$$H^{\rm iso}_{\rm QR}(\gamma) \approx \frac{\pi}{2}\;(\sin\alpha)^{2/3}\,(\gamma u)^{4/3}\,. \tag{136}$$

Accounting for the slightly different definitions of $H^{\rm iso}(\gamma)$ and $K^{(h)}_{\rm QR}(\sigma)$ in equations (33) and (121), the results in equations (136) and (124) are entirely equivalent since at fixed γ the QR domain is concentrated near $\varpi=0$ at $\sigma=\gamma u\sin^2\!\alpha$. This was not unexpected because the QR domain is of a very small angular extent, so that the QR contribution is insensitive to the fact that the distribution function is isotropic or otherwise. Finally, the asymptotic expansion in γ of the first term in equation (131), limited to the order $\gamma^{4/3}$, is

$$-\frac{\pi}{2}\,\sin^2\!\alpha\,\left(\gamma\,(2\gamma^2-3)\,\sqrt{\gamma^2-1}+\mathcal{L}(\gamma)\right)\approx-\frac{\pi}{2}\,\sin^2\alpha\,(2\gamma^4-4\gamma^2)\,. \tag{137}$$

The complete $H^{\rm iso}(\gamma)$ kernel in the LF limit is the sum of the three contributions in equations (134), (136) and (137). The large terms proportional to γ^4 and γ^2 cancel out and the net result, valid in the LF limit, is:

$$H^{\rm iso}_{\rm LF}(\gamma) \approx \frac{\pi}{8}\,(\gamma u)^{4/3}\,(\sin\alpha)^{2/3}\left(4-\frac{1}{3^{4/3}}\right)\,. \tag{138}$$

This result is in complete agreement with those in equation (124) and confirms that in the LF limit neither the resonant nor the NR contribution to h predominates.

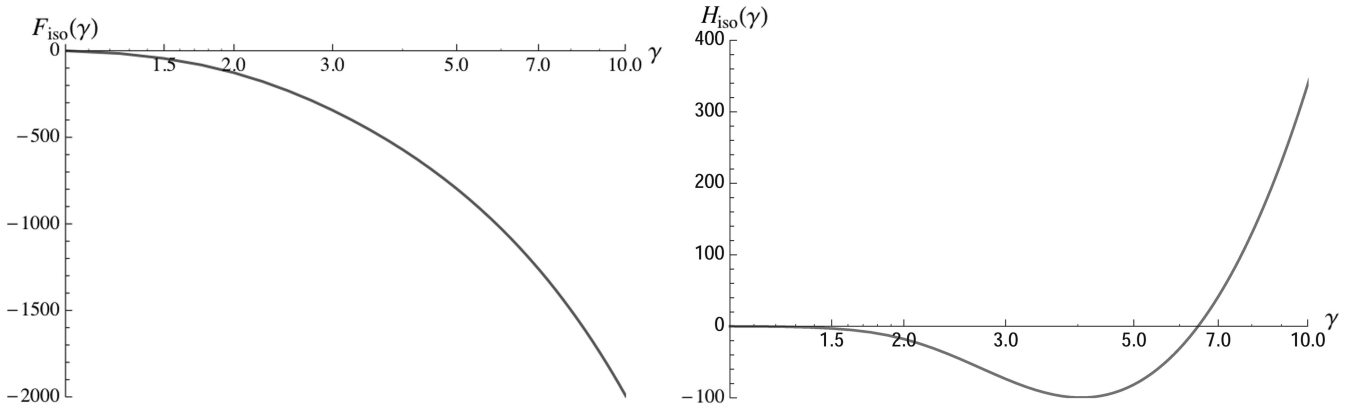

Figure 8. The isotropic kernels $F^{\rm iso}(\gamma)$ (left-hand panel) and $H^{\rm iso}(\gamma)$ (right-hand panel) as given by equations (125) and (126). The parameters of the radiation are $\omega = 15|\Omega|$ and $\alpha = \pi/4$.

6.5 Approximate expressions for the isotropic kernels over the full energy range

Equations (38) and (39) provide expressions for the isotropic kernels in the HF regimes that are valid in the interval $[1, \gamma_{\rm QR}]$, although when γ approaches $\gamma_{\rm QR}$ from below more terms should be retained in the Debye expansion. Equations (130) and (138) provide expressions of the kernels in the asymptotic LF regime at $\gamma \gg \gamma_{\rm QR}$. The transition between the HF regime and the asymptotic LF regime should take place over an interval $\gamma_{\rm QR1} < \gamma < \gamma_{\rm QR2}$, where $\gamma_{\rm QR1} = A_1\gamma_{\rm QR}$ and $\gamma_{\rm QR2} = A_2\gamma_{\rm QR}$ and $A_1 < 1$ and $A_2 > 1$ are coefficients of order unity. For the kernel $F^{\rm iso}(\gamma)$, these coefficients should be close to unity because the change from the HF regime to the LF regime for this coefficient is dim. For $H^{\rm iso}(\gamma)$, or its derivative $H'^{\rm iso}(\gamma)$, A_2 is more likely to be of the order of several units since Fig. 7 shows that the asymptotic regime is in this case slowly reached. Fig. 8 shows that exact kernels are continuous and at least once differentiable. Our proposed approximation adopts the HF expressions (38) and (39) at $\gamma < \gamma_{\rm QR1}$ and extends them into the LF domain by a function that connects at $\gamma_{\rm QR1}$ to the HF expression and to its first-order derivative and asymptotically merges into the LF limit in equation (130) or (138). The kernels themselves or their derivatives could be interpolated that way, according to whether one wishes to use equation (33) as they stand or to calculate them by integrating by parts. We opted for the second method for the coefficient h, which minimizes the inaccuracies due to the existence of singularities in the derivative of the distribution functions of truncated power laws. We interpolate from $\gamma_{\rm QR1}$ to infinity by connection functions $C_{ci}(\gamma - \gamma_{\rm QR1})$ that we define for coefficient c (=f or h) and element i in the connection ($i = 1$ for HF and $i = 2$ for LF) by

$$C_{ci}(\gamma - \gamma_{\rm QR1}) = \left(1 - \exp\left(-\frac{(\gamma - \gamma_{\rm QR1})}{\lambda_{ci}\,\gamma_{\rm QR1}}\right)\right)^2 . \tag{139}$$

The fact that this function is a square warrants that the interpolated function and its first derivative are continuous at $\gamma_{\rm QR1}$ when the functions to be joined are themselves continuously dfferentiable. The extrapolations of the HF expressions to the LF domain that appear in the second lines of equations (140) and (141) must then be continuous and derivable at $\gamma_{\rm QR1}$ but are otherwise unconstrained. A linear extrapolation proved satisfactory for $F^{\rm iso}$, taking in this case $\gamma_{\rm QR1} = \gamma_{\rm QR2} = \gamma_{\rm QR}$. Due to the non-negligible gap that the interpolation should bridge between the HF and the LF regime, the interpolation formula for the derivative $H'^{\rm iso}(\gamma)$ of the kernel of the h coefficient is more sophisticated. A value of $\gamma_{\rm QR1}$ smaller than $\gamma_{\rm QR}$ has been chosen, and the extrapolation of the HF behaviour in the LF domain at $\gamma > \gamma_{\rm QR1}$ has been endowed with a local bump that is meant to represent the cumulative effect of higher order terms in the Debye expansion when approaching its limit of validity.

The decrement parameter λ_{ci} is a constant, chosen to optimize the fit to the exact kernels in Fig. 8. For the kernel $F^{\rm iso}$ we have adopted $\lambda_{f1} = \lambda_{f2} = 1/(1.7)$. For the derivative $H'^{\rm iso}(\gamma)$ of the kernel of h we have adopted $\gamma_{\rm QR1} = 0.7\gamma_{\rm QR}$ and different decrement parameters λ_{ci} in equation (139), namely $\lambda_{h1} = 0.4$ and $\lambda_{h2} = 1.8$. Other relevant parameters are described below. The resulting interpolation formulae for $F^{\rm iso}(\gamma)$ and $H'^{\rm iso}(\gamma)$ at $\gamma > \gamma_{\rm QR1}$ are

$$F^{\rm iso}_{\rm int}(\gamma) = \pi s_q u \cos\alpha \left[C_f(\gamma - \gamma_{\rm QR})\,\gamma\left(\frac{4}{3}\ln\left(\frac{\gamma u}{\sin\alpha}\right) - 1.260\,724\,39\right) + \left(1 - C_f(\gamma - \gamma_{\rm QR})\right)\right.$$
$$\left. \times \left(4\gamma_{\rm QR}\ln\left(\gamma_{\rm QR} + \sqrt{\gamma_{\rm QR}^2 - 1}\right) - 4\sqrt{\gamma_{\rm QR}^2 - 1} + 4\ln\left(\gamma_{\rm QR} + \sqrt{\gamma_{\rm QR}^2 - 1}\right)(\gamma - \gamma_{\rm QR})\right)\right], \tag{140}$$

$$H'^{\rm iso}_{\rm int}(\gamma) = C_{h2}(\gamma - \gamma_{\rm QR1})\left(-\frac{\pi}{6}\left(u^2\sin\alpha\right)^{2/3}\left(4 - \frac{1}{3^{4/3}}\right)\gamma^{1/3}\right) + \left(1 - C_{h1}(\gamma - \gamma_{\rm QR1})\right)$$
$$\times\ \frac{\pi\,\sin^2\alpha}{2}\left[4(2\gamma_{\rm QR1}^2 - 1)\sqrt{\gamma_{\rm QR1}^2 - 1} + \frac{4(6\gamma_{\rm QR1}^2 - 5)\gamma_{\rm QR1}}{\sqrt{\gamma_{\rm QR1}^2 - 1}}\,(\gamma - \gamma_{\rm QR1}) + \eta\,\frac{\left(\frac{\gamma - \gamma_{\rm QR1}}{\mu\gamma_{\rm QR1}}\right)^2}{1 + \left(\frac{\gamma - \gamma_{\rm QR1}}{\mu\gamma_{\rm QR1}}\right)^3}\right]. \tag{141}$$

The coefficient $\eta = 103$ and $\mu = \lambda_{h1}/1.5$. The transition value $\gamma_{\rm QR}$ rigorously is the value of γ that causes the line of constant γ in Fig. 6 to tangent the NR–QR boundary. It slightly differs from the γ value associated with $\sigma_{\rm QR}$ at $\varpi = 0$ that is approximately representative of it and to which it reduces for $\cos\alpha = 0$. In our numerical evaluations we used the exact value, given by

$$\gamma_{\rm QR}\, u \sin^2\alpha = \sqrt{\frac{u\sin\alpha}{3}}\ \left(u\sin\alpha - \cos^2\alpha\right). \tag{142}$$

In Appendix L we give some examples of Faraday coefficients derived from the interpolating formulae (140) and (141) and contrast them with the quasi-exact ones obtained by double integration over ϖ and σ of the expressions in equations (25) and (26). The accuracy of the fit provided by the interpolating formulae is of the order of or better than about 10 per cent in this frequency range.

7 CONCLUSION

7.1 Summary of the results in the different regimes

We have derived an almost exact expression for the Faraday transfer coefficients in the form of equations (25) and (26), which we repeat here, as expressed in terms of the ϖ–σ variables defined in equation (23):

$$f = -\frac{2\pi^2 s_q}{c}\ \frac{\omega_{\rm pr}^2\Omega^2}{\omega^3}\iint \frac{m^3c^3}{\sin^2\alpha}\,{\rm d}\varpi\,{\rm d}\sigma\ \ \varpi\, x\ \frac{\partial F_0}{\partial\sigma}\ \left[J'_\sigma(x)N_\sigma(x) + \frac{1}{\pi x}\right], \tag{143}$$

$$h = \frac{\pi^2}{c}\frac{\omega_{\rm pr}^2\Omega^2}{\omega^3}\iint \frac{m^3c^3}{\sin^2\alpha}\,{\rm d}\varpi\,{\rm d}\sigma\left[\frac{\partial F_0}{\partial\sigma}\left(x^2J'_\sigma(x)N'_\sigma(x) - \varpi^2 J_\sigma(x)N_\sigma(x)\right) + \frac{1}{\pi}\left(\varpi\frac{\partial F_0}{\partial\varpi} - \sigma\frac{\partial F_0}{\partial\sigma}\right)\right]. \tag{144}$$

These expressions, which involve a two-real-variables integration, are completely general, applying to isotropic as well as to non-isotropic distributions and encompassing all regimes of particle–wave interaction. The Olver uniform expansions of high-order Bessel functions presented in Appendix G can be used to speed up the integration in equations (143) and (144) when very high values of σ are considered. In the HF limit, when QR contributions to these integrals are negligible, the transfer coefficients can be more simply written as

$$f_{\rm HF} = 2\pi s_q\,\frac{\omega_{\rm pr}^2\Omega^2}{c\,\omega^3}\iint\ \frac{m^3c^3}{\sin^2\alpha}\,{\rm d}\varpi\,{\rm d}\sigma\ \ \left(\frac{1}{2}\,\frac{\varpi x^2}{(\sigma^2-x^2)^{3/2}}\right)\frac{\partial F_0}{\partial\sigma}, \tag{145}$$

$$h_{\rm HF} = -\,\pi\,\frac{\omega_{\rm pr}^2\Omega^2}{c\,\omega^3}\iint\ \frac{m^3c^3}{\sin^2\alpha}\,{\rm d}\varpi\,{\rm d}\sigma\ \ \left(\frac{1}{8}\,\frac{2x^4(\sigma^2-x^2)+\sigma_0^2x^2(4\sigma^2+x^2)}{\left(\sigma^2-x^2\right)^{7/2}}\right)\frac{\partial F_0}{\partial\sigma}. \tag{146}$$

Within the HF limit, these expressions are also completely general. The integrands in equations (145) and (146) are more regular than those in equations (143)–(146). The integration over ϖ in equations (145) and (146), although it is meant to cover the NR domain only, extends in the HF limit to the full physical domain by lack of a QR contribution, the QR domain then being ill-populated.

We have particularized equations (145) and (146) to a number of different physical situations. For isotropic distribution functions they reduce to equations (38) and (39), which coincide with known results for thermal distribution functions, as shown in Section 3.2.4. A quadrupolar anisotropy, represented by a distribution function as in equation (51), produces the transfer coefficients shown in equations (53) and (54) while anisotropies of higher multipolar orders generate the coefficients compiled in Appendix I. In all these cases, the expression of the transfer coefficients is reduced to a one-variable quadrature over the energy of the particles. For anisotropies that cannot be expanded in a sum of a few multipolar terms, the HF coefficients are obtained by performing the double integrals in equations (145) and (146), either in these variables or in others, as shown in the case of a beam in Section 3.3.2.

The HF approximation progressively loses validity as the fraction of particles with a Lorentz factor γ large enough to interact with the wave in the LF mode increases. A regime change occurs when the QR contribution ceases to be negligible, which, for a given frequency and a given direction of propagation, happens for Lorentz factors such that their characteristic synchrotron frequency, defined in equation (101), is of the order of or larger than the frequency of the radiation considered. We offer clear physical and mathematical explanations for this behaviour, that has been previously well observed in the results of Shcherbakov (2008) and Huang & Shcherbakov (2011): the regime change occurs when particles in quasi-resonance make a contribution comparable to the NR one. From a mathematical standpoint, the two-variable kernels in equations (143) and (144) must be represented differently in these two regimes, in terms of Nicholson's approximations for quasi-resonance or in terms of the Debye expansion of high-order Bessel functions for non-resonance.

In full generality, the QR contributions to the transfer coefficients are given by equations (99) and (100). The QR contribution to h is however better expressed as in equation (120). When QR contributions are important, the NR and QR contributions should eventually be added and care should be taken to integrate the QR contributions in equations (99) and (120) over the QR domain only and the NR contributions in equations (145) and (146) over the NR domain only. We have compared the QR and NR contributions to the Faraday coefficients in Section 5.4, and shown that in the LF limit none of them predominates. For a given frequency, the QR contribution to the Faraday conversion coefficient h grows when $\sigma \gg \sigma_{\rm QR}$ to a value comparable to, and in fact numerically larger than, the NR one. In the limit of large energies, the angular integration over the QR domain covers a very small interval in pitch angle space, as can be seen from equation (91). Across this

interval, the partial derivative $\partial_\sigma F_0$ usually varies by only a little amount. Our estimation in Section 5.4 of $\hat{h}_{\rm QR}$ is for this reason expected to be a reliable one, that can be written in the LF limit as

$$\hat{h}_{\rm LF}^{\rm QR} = \frac{\omega_{\rm pr}^2 \Omega^2}{c\,\omega^3} \int_{\sigma \gg \sigma_{\rm QR}}^{\infty} \frac{m^3 c^3}{\sin^2\alpha}\,{\rm d}\sigma\ \ \frac{\pi}{2}\,\sigma^{4/3}\,\partial_\sigma F_0(\varpi = 0, \sigma)\,. \tag{147}$$

Equation (147) is one among different contributions to h. It is meant to apply only to values of σ that are relevant to the asymptotic LF limit. It is otherwise general and valid for any distribution function whatever the pitch angle distribution, the latter being anyway irrelevant to the QR contribution.

The complication of accounting for both NR and QR contributions has been overcome for isotropic distribution functions by actually calculating their sum in the LF limit. This has led to the results in equations (33), (130) and (138). The asymptotic LF contribution to the Faraday coefficients is in this case

$$f_{\rm LF}^{\rm iso} = \pi s_q \frac{\omega_{\rm pr}^2\,|\,\Omega\,|}{c\,\omega^2}\,\cos\alpha \int_{\gamma \gg \gamma_{\rm QR}}^{\infty} m^3 c^3\,{\rm d}\gamma\,\gamma \left(\frac{4}{3}\ln\left(\frac{\gamma u}{\sin\alpha}\right) - 1.260\,724\,39\right)\,\frac{{\rm d}F_0}{{\rm d}\gamma}\,, \tag{148}$$

$$h_{\rm LF}^{\rm iso} = \frac{\omega_{\rm pr}^2\,|\,\Omega\,|^{2/3}}{c\,\omega^{5/3}}\,\sin\alpha^{2/3}\,\frac{\pi}{8}\left(4 - \frac{1}{3^{4/3}}\right) \int_{\gamma \gg \gamma_{\rm QR}}^{\infty} m^3 c^3\,{\rm d}\gamma\,\gamma^{4/3}\,\frac{{\rm d}F_0}{{\rm d}\gamma}\,. \tag{149}$$

These simple analytical results, which apply to the asymptotic LF regime $\gamma \gg \gamma_{\rm QR}$, do not seem to have appeared so far in the literature. For example, Shcherbakov (2008) and Huang & Shcherbakov (2011) provide intermediate and low-frequency regime fits to numerical results. For application to specific distributions functions, equations (25) and (26), (31) and (32), (145) and (146) or (147) may of course be expressed in terms of any set of physical variables, such as the Lorentz factor γ and pitch angle ϑ of the particles, as was partly done in Sections 3.2 and 3.3.

We proposed in equations (140) and (141) approximate expressions of the kernels of the Faraday coefficients for isotropic distribution functions that interpolate between the HF regime and the asymptotic LF one. These approximations to the kernels generate reasonably accurate expressions of the coefficients f and h that can be written in the form of a simple one-variable quadrature over the entire energy range. In the HF limit, we have similarly reduced to a one-variable quadrature on energy the expression of the Faraday coefficients for a large class of anisotropic distribution functions proportional to Legendre polynomials of low degree depending on the cosine of the pitch angle. These functions may be used as a basis for expanding distribution functions of any simple kind of anisotropy. For distribution functions with sharp anisotropies, our results can be made completely explicit by performing a double integration over energy and angle.

7.2 Discussion and prospects

Our analytical results have been deduced from a new, but straightforward, calculation of the anti-Hermitian part of the conductivity tensor expressed in a form in which the usual sum over discrete synchrotron resonances is exactly replaced by an integration over a continuous variable. This particular representation of the conductivity tensor has not been hitherto used in this context. The integral over this continuous variable has principal value singularities that can be exactly reduced to the sum of a regular part and of a residual part that has been shown to be safely negligible. As a result, simple, general, quasi-exact and non-singular expressions for the transfer coefficients have been obtained in a form that parallels that of the familiar expressions of the synchrotron emission and absorption coefficients, but differs from the form in which Faraday coefficients are usually expressed in the literature. Notwithstanding this difference our results exactly coincide with known exact ones for thermal distributions.

Unlike the Hermitian part of the conductivity, which describes synchrotron absorption, the anti-Hermitian part is never dominated by the contribution of a small QR population travelling close to the direction of propagation of the considered wave. On the contrary, NR particles make most of the contribution to the non-dissipative coefficients in the HF limit and cannot be ignored otherwise.

The transfer properties of relativistic plasmas may sensibly differ from those of cold plasmas, which may be a useful diagnostic. For example, the Faraday rotation coefficient f of a symmetric pair plasma, with equal densities of electrons and positrons having identical distribution functions, exactly vanishes but its Faraday conversion coefficient h does not. The study of a field-aligned beam in Section 3.3.2 also revealed that the Faraday rotation coefficient is enhanced in this case for radiation travelling in the beam. The knowledge of transport coefficients in all physical regimes, HF or LF, should allow optimal use of inversion algorithms of multiwavelength polarization data to yield the density and magnetic structure of the source and of the intervening medium.

The reconstruction of the magnetic field distribution in volume, from multiwavelength polarization observations of synchrotron emitting astrophysical media, has been attempted either partially (‘Faraday synthesis’; Brentjens & de Bruyn 2005) or fully (Thiébaut et al. 2010), but in the latter case assuming a known distribution of the electronic population(s) responsible for the synchrotron emission and/or the Faraday rotation. In the case of cold plasmas (e.g. the interstellar medium of our Galaxy or nearby galaxies) where the circular polarization is negligible (both from emission and transfer), these assumptions about the underlying electronic spatial distribution(s) are a real limitation to reconstructing the magnetic field structure. However, it was also shown (Thiébaut et al. 2010) that in the case of relativistic sources where a single electronic distribution would be responsible for both synchrotron emission and radiative transfer effects (through their contribution to the dielectric properties of the plasma), the multiwavelength observation of circular polarization (in addition to intensity and linear polarization)

should in principle allow the simultaneous reconstruction of the magnetic field *and* electronic spatial distributions. In this context, the Faraday rotation and conversion coefficients derived in this work are of particular interest. The diagnostic of relativistic jets from galactic nuclei and of pulsar winds by these methods would be of particular interest. It should be noted however that our present results only yield the transfer coefficients in the plasma rest frame and should be transformed to the observer's frame for use in the inversion algorithm for example along the lines described by Gammie & Leung (2012).

ACKNOWLEDGEMENTS

We thank M. Lemoine and G. Pelletier for early discussions and the 'Programme National de Cosmologie et Galaxies' for funding. CP thanks the community of http://mathematica.stackexchange.com for technical advice.

REFERENCES

Abramowitz M., Stegun I., 1964, National Bureau of Standards, Handbook of Mathematical Functions, 2nd edn. US Government Printing Office, Washington, DC
Agol E., 2000, ApJ, 538, L21
Beck R., 2009, Rev. Mex. Astron. Astrofis., 36, 1
Beckert T., 2003, Ap&SS, 288, 123
Bekefi G., 1966, Radiation Processes in Plasmas. Wiley, New York
Bicknell G. V., Jones D. L., Lister M., 2004, New Astron. Rev., 48, 1151
Brentjens M. A., de Bruyn A. G., 2005, A&A, 441, 1217
Carilli C. L., Rawlings S., 2004, New Astron. Rev., 48, 979
Cioffi D. F., Jones T. W., 1980, AJ, 85, 4
Dewdney P. E., Schilizzi R. T., Lazio T. J. L. W., 2009, Proc. IEEE, 97, 8
Dovciak M., Muleri F., Goosmann R. W., Karas V., Matt G., 2008, MNRAS, 391, 32
Dyks J., Harding A. K., Rudak B., 2004, ApJ, 606, 1125
Feretti L., Johnston-Hollitt M., 2004, New Astron. Rev., 48, 1145
Gaensler B. M., Beck R., Feretti L., 2004, New Astron. Rev., 48, 1003
Gammie C. F., Leung P. K., 2012, ApJ, 752, 123
Ginzburg V. L., Sirovatskii S. I., 1969, ARA&A, 7, 375
Heyvaerts J., 1969, Ap&SS, 5, 36
Heyvaerts J., 1970, thesis, Faculté des Sciences de Paris
Homan D. C., Wardle J. F. C., 2004, ApJ, 602, L13
Huang L., Shcherbakov R., 2011, MNRAS, 416, 2574
Ichimaru S., 1973, Basic Principles of Plasma Physics, Frontiers in Physics Series. Benjamin, Reading, MA
Jones T. W., O'Dell S. L., 1977, ApJ, 214, 522
Kanbach G., Kellner S., Schrey F. Z., Steinle H., Straubmeier C., Spruit H. K., 2003, Proc. SPIE, 4841, 82
Matviyenko G., 1992, Research Report of Yale University, Department of Computer Science, YALEU/DCS/RR-903
Mc Donald J., O'Connor P., de Burca D., Golden A. Shearer A., 2010, MNRAS, 417, 730
Melrose D. B., 1997a, J. Plasma Phys., 57, 479
Melrose D. B., 1997b, J. Plasma Phys., 58, 721
Melrose D. B., 1997c, J. Plasma Phys., 58, 735
Melrose D. B., 1997d, Phys. Rev. E, 56, 3527
Montgomery D. C., Tidman D. A., 1964, Plasma Kinetic Theory. McGraw-Hill, New York
Olver F. W. J., 1952, Math. Proc. Camb. Phil. Soc., 48, 414
Olver F. W. J., 1954, Phil. Trans. R. Soc. A, 247, 328
Petiau G., 1955, La Théorie des Fonctions de Bessel. Editions du CNRS, Paris
Petri J., Kirk J., 2005, ApJ, 627, L37
Qin H., Phillips C. K., Davidson R. C., 2007, Phys. Plasmas, 14, 092103
Ramaty R., 1968, J. Geophys. Res., 11, 3573
Razin V. A., 1960, News of Higher Educational Institutions, Ministry of Higher Education, Radio Physics Series, 3, 73
Sazonov V. N., 1969a, SvA, 13, 396
Sazonov V. N., 1969b, Sov. Phys. – JETP, 29, 578
Sazonov V. N., Tsytovitch V. N., 1968, Radiofisika, 11, 1287
Shcherbakov R. V., 2008, ApJ, 688, 695
Shcherbakov R. V., 2011, PhD thesis, Harvard University
Shcherbakov R. V., Huang L., 2011, MNRAS, 410, 1052
Stirling A. M., Spencer R. E., Cawthorne T. V., Paragi Z., 2004, MNRAS, 354, 1239
Swanson D. G., 2002, Plasma Phys. Control. Fusion, 44, 1329
Thiébaut J., 2010, thesis, Université Pierre et Marie Curie, Paris
Thiébaut J., Prunet S., Pichon C., Thiébaut E., 2010, MNRAS, 403, 415
Trubnikov B. A., 1958, PhD thesis, Moscow Inst. Engineering and Physics
Tsytovitch V. N., 1951, Vestnik Moscow Univ. 6, No. 11, Ser. Fiz.-Mat. Estestven. Nauk, 7, 27
Watson G. N., 1922, The Theory of Bessel functions. Cambridge Univ. Press, Cambridge
Westfold K. C., 1959, ApJ, 130, 241
Wild J. P., Weiss A. A., Smerd S. F., 1963, ARA&A, 1, 291

Yuen R., Manchester R. N., Burgay M., Camillo F., Kramer M., Melrose D. B., Stairs J. H., 2012, ApJ, 752, L32
Zheleznyakov V. V., 1967, Sov. Phys. – JETP, 24, 381
Zheleznyakov V. V., Suzorov E. V., Shaposhnikov V. E., 1974, SvA, 18, 142

SUPPORTING INFORMATION

Additional Supporting Information may be found in the online version of this article:

APPENDIX A: VARIABLES SUITED TO THE RELATIVISTIC PARTICLE-WAVE INTERACTION
APPENDIX B: THE CONTINUOUS-SPECTRUM REPRESENTATION OF THE CONDUCTIVITY
APPENDIX C: THE DISTRIBUTION ASSOCIATED WITH MULTIPLE RESONANCES
APPENDIX D: THE TRANSVERSE COMPONENTS OF THE CONDUCTIVITY
APPENDIX E: RESIDUAL PRINCIPLE VALUE TERMS ARE NEGLIGIBLE
APPENDIX F: NICHOLSON'S APPROXIMATION
APPENDIX G: OLVER UNIFORM ASYMPTOTIC EXPANSION OF BESSEL FUNCTIONS
APPENDIX H: COMPARISON OF QUASI-RESONANT AND NON-RESONANT CONTRIBUTIONS
APPENDIX I: KERNELS OF HIGHER MULTIPOLAR ORDERS FOR FARADAY COEFFICIENTS AT HIGH-FREQUENCY
APPENDIX J: FARADAY CONVERSION COEFFICIENT IN THE LOW-FREQUENCY LIMIT
APPENDIX K: FARADAY ROTATION COEFFICIENT IN THE LOW-FREQUENCY LIMIT
APPENDIX L: TRANSFER COEFFICIENTS FROM INTERPOLATED ISOTROPIC KERNELS (http://mnras.oxfordjournals.org/lookup/suppl/doi:10.1093/mnras/stt135/-/DC1).

Please note: Oxford University Press are not responsible for the content or functionality of any supporting materials supplied by the authors. Any queries (other than missing material) should be directed to the corresponding author for the article.

This paper has been typeset from a TEX/LATEX file prepared by the author.